Faculty of Science and Technology

Department of Physics and Technology

Smart Senja electrical network expansion modeling

Oskar Marthinussen

EOM-3091 Master thesis in energy, climate and environment - June 2023

Abstract

The addition of variable renewable energy sources into the electrical energy systems of the world has been increasing in recent years. This form of distributed energy production with high production volatility can introduce massive challenges in operating a lower voltage distribution network. One of these affected networks is on the island of Senja in northern Norway, with an eldering radial electrical network with a single connection to the national transmission grid. In this study, prescriptive analysis of the network through mathematical optimization is implemented to investigate if there are more effective solutions to this problem other than building more electrical lines. In selected parts of the island, the electrical network experiences electrical faults of different magnitude and concern affecting 1500 hours a year. In this thesis, the model GenX is presented which prescribes solutions reducing these faults to zero while also cutting costs compared to the baseline scenario of today's system. Results from the model indicate that simple installments of distributed power generation in conjunction with electrical energy storage drastically improve network capacity and industrial expansion opportunities. Also investigated is the feasibility of operating the electrical network on the island without any connection to the external grid. Meant as a proof of concept for the application of mathematical optimization on electrical grids in other more remote parts of the world. The model proves that investments in local electricity production positively impact the system at a fraction of the cost of building new regional distribution infrastructure. Finally, some drawbacks of the chosen analytical tool used to construct the mathematical optimization model are presented alongside selected methods applicable to apprehend or circumvent these limitations.

Acknowledgments

Table of Contents

List of Tables

List of Figures

1 Introduction

1.1 Background

Electricity consumption in Norway has risen by 14.6% between 1990 and 2020, while electric energy production has increased by 26.5% in the same period, with hydropower plants accounting for 90% of the country's power production [1]. In recent years there is a shift towards installing variable renewable energy (VRE) technologies, implementing renewable distributed generation has become increasingly necessary, which needs a high level of control in the distribution networks. Although renewable energy sources have positive environmental impacts, they also present challenges regarding required electrical grid stability. There is an increased focus on developing the distribution system to accommodate new renewable electricity generation capabilities. The ongoing Smart Senja project led by Troms Kraft is an example of this, which aims to develop the distribution system by implementing alternative technologies, compared to traditional grid expansion [2]. The coastal community at Senja is experiencing limitations in the electrical network due to increasing energy consumption from expansions in the seafood industry, which is expected to jeopardize the stable operation of the power system if measures are not taken. The 22 kV distribution network features long radials, making the consumers at the endpoints susceptible to low network voltages during heavy load or low power production during months of scarce water [3]. This poses a risk of unstable and inadequate power supply with critical consequences for industrial establishments that rely on stable and secure power. In the worst case, the sea cable can experience a complete failure and leave the island to produce all its electrical power, as almost was the case before the cable was upgraded last year. The distribution networks are at their limits during the wild-caught fishery high season, especially from January to April. An industrial expansion is necessary to meet the global demand for seafood, but the electrical network capacity issues limit the expansion rate [4]. Hydropower plants located along these vulnerable radials are crucial to maintaining a satisfactory voltage level, but other measures must be implemented to meet the future demand for reliable power.

Earlier studies conducted through the Smart Senja project and the research group Renew include a comprehensive arrangement of opportunities for electrical network stability improvements while discussing some of the problems of the existing distribution network. Some master theses within the project have assessed methods of improvement, including shunt capacitor reactive compensation and distributed power production in selected areas [5, 6]. Assessments of the pumped hydro energy storage potential in the network have been conducted [7]. Papers published through the project have assessed predictions of electricity demand in the area and predictions of electrical faults in the distribution network [8-10]. Before the project was initiated a preliminary study was conducted as a part of conceiving the project and applying for financial support through the politically governed company Enova [3].

1.2 Scope of Study

The Smart Senja project seeks to implement a large-scale demonstration of smart infrastructure that strengthens the security of supply in a vulnerable distributional network. This project mainly focuses on two selected communities in the island's northern part. Still, the underlying research group Renew is interested in conducting a more comprehensive study of the entire island.

With modern mathematical optimization tools such as GenX, the chosen tool for this thesis, a one-shop method can be implemented to study a wide range of aspects regarding upgrading and maintaining an electrical power system. As prescriptive analytics through mathematical optimization can provide excellent foresight into future problem-solving, a scenario-based study has been constructed to highlight some key features of this groundbreaking tool.

The selected scenarios want to investigate alternative solutions to building more power distribution capacity. Through distributed local power generation and modern electrical energy storage solutions, the model seeks to examine the inherent power balance in the network and test if the current distribution network can be utilized further into the future. Also tested is the island operation capacity of the regional distribution network on Senja.

Finally, the thesis aims to showcase the capabilities of the free, open-source, and powerful tool for electrical system modeling and to what degree the tool is capable of small-scale case studies such as this.

1.3 Outline of the Thesis

This thesis is divided into the following five chapters:

- **Chapter 1** – Introduction to the thesis with motivation and scope of the thesis.

- **Chapter 2** – Theoretical background on subjects related to the study and presentation of relevant electrical machinery within a typical Nordic electrical network.

- **Chapter 3** – Method and Data used to conduct the study included in the thesis. The method consists of a presentation of the mathematical optimization tool used to simulate the electrical network and a display of how the relevant electrical machinery presented in the theory is modeled through this tool. Data handling and input configuration are also described in detail.

- **Chapter 4** – Results found through the study with a presentation and discussion of the importance of these. Limitations of the study are also presented, with an emphasis on limitations within the modeling software and the modeling decisions made.

- **Chapter 5** – Conclusion with final remarks on the results and their significance. Also presented are some suggestions for further study within the field of the thesis.

2 Theory

2.1 Electrical Power Generation

Renewable energy production expansion is one of the driving factors in meeting the $1.5°C$ target in the Paris Agreement. In later years large efforts have been exerted to diverge the world's energy mix from its current dependence on fossil fuels to a more sustainable solution [11]. As seen in Figure 2-1 large amounts of renewable sources have been constructed during the previous years, and thankfully this trend is still growing. As mentioned in Chapter 1.1, Norway has also been expanding its electrical power capacity substantially in recent years, with a large part of this being hydroelectric or wind generators.

At large one can differentiate clean renewable power generation into two separate categories. One category is the controllable resources comprised largely of hydroelectric power generation presented in Chapter 2.1.1 and implemented in Chapter 3.2. The other category is VRE sources with many popular technologies. In this thesis, VRE will be comprised of photovoltaic (PV) solar power and wind power. Presented in Chapters 2.1.2 and 2.1.3, and implemented in Chapter 3.2. Directly correlated to variable energy sources are power balancing measures such as electric energy storage and other similar balancing technologies. Presented in Chapter 2.3.1 and implemented in Chapter 3.2.1. These technologies are paramount for high VRE penetration as an electrical grid is structured to always balance supply and demand, and this balance can be implemented through variable sources in conjunction with storage.
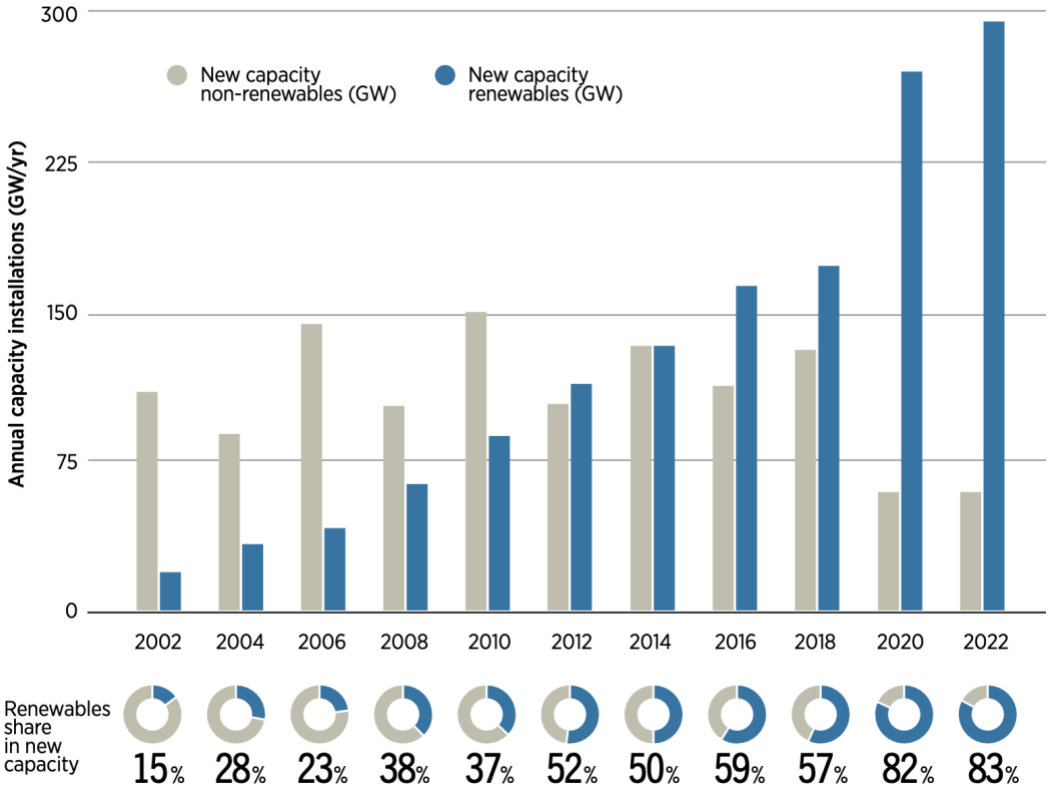
Figure 2-1 Annual power capacity expansion in the world, 2002-2022 [IRENA, 2023]

2.1.1 Hydropower

Hydroelectric power production is a method of generating electricity using the energy of flowing water [12]. It is one of the most widely used forms of renewable energy and is responsible for approximately 16% of the world's electricity generation [13]. Hydroelectric power plants convert the kinetic energy of water into electrical energy by using turbines that spin generators.

The process of hydroelectric power production begins with the construction of a dam. The dam is typically constructed across a river or other water source to create a reservoir. The reservoir created by the dam is called an impoundment. When water is released from the impoundment, it flows through a penstock, a large pipe or tunnel, and is directed towards the turbine. The force of the water flowing through the penstock turns the turbine's blades, causing it to spin. The spinning turbine then powers the generator, which converts the turbine's mechanical energy into electrical energy [12].

One of the advantages of hydroelectric power production is that it is a clean and renewable energy source. Unlike fossil fuels, which produce greenhouse gases and contribute to climate change, hydroelectric power plants do not produce emissions. Hydroelectric power plants have a long lifespan and can operate for up to 100 years or more with proper maintenance [14].

Another advantage of hydroelectric power production is that it is highly efficient. Hydroelectric power plants can convert up to 90% of the energy from the flowing water into electricity, much higher than other forms of renewable energy such as wind and solar power [12, 15, 16]. Hydroelectric power plants also have a high level of reliability and can operate continuously, providing a consistent energy source [17].

There are several types of hydroelectric power plants, each with unique advantages and disadvantages. The most common type of hydroelectric power plant is a conventional one, which uses a dam to create an impoundment of water. Traditional hydroelectric power plants are highly controllable and can generate a large amount of electricity. Still, they can also have negative environmental impacts, such as altering the natural flow of rivers and affecting fish populations [18].

Another type of hydroelectric power plant is pumped storage, which uses surplus energy to pump water from a lower reservoir to a higher reservoir. When electricity is needed, the water is released from the upper reservoir and flows through a turbine to generate electricity [19]. Pumped-storage hydroelectric power plants are highly efficient and can store excess energy from renewable sources such as wind and solar.

Run-of-river hydroelectric power plants are another type of hydroelectric power plant that does not require dam construction. Instead, these power plants use the natural flow of a river to generate electricity [17]. Run-of-river hydroelectric power plants have a smaller environmental impact than conventional ones [18]. Still, they are less efficient and can only generate electricity when there is sufficient water flow in the river [12]. In addition to producing electricity, hydroelectric power plants can also provide other benefits. For example, some hydroelectric power plants are used for irrigation, flood control, and navigation [18]. Hydroelectric power plants can also provide drinking water and recreation opportunities like boating and fishing.

Despite its many advantages, hydroelectric power production also has some disadvantages. One of the main disadvantages is the environmental impact of building dams and impoundments. The construction of dams can alter the natural flow of rivers and affect fish populations, and the creation of impoundments can flood large areas of land and displace people and wildlife [18].

Another disadvantage of hydroelectric power production is that it can be affected by droughts and other weather conditions that affect the water supply. During droughts, water levels can drop below the level required to generate electricity, leading to power shortages [14].

2.1.2 Solar Power

Solar power is a variable renewable energy source that has gained significant attention in recent years due to its potential to reduce greenhouse gas emissions and combat climate change [13]. Solar power production generates electricity from sunlight using a wide variety of technology where we can differentiate between direct and indirect methods. Within both methods extensive research has been carried out in the year both from a technology and economic point of view [20-22]. Silicon based PV is a direct electricity generating technology that involves converting the energy from sunlight into electricity to power homes, businesses, and industries [23, 24]. Silicon based PV has become the most affordable form of electricity production in the world [13, 25, 26].

The essential components of a solar power production system include solar panels, inverters, and batteries. Solar panels are made up of PV cells that convert sunlight into DC electricity. The inverter converts the DC electricity into alternating current (AC) electricity that can be used to power homes and businesses [16, 23]. The batteries store excess energy generated during the day for use at night or during periods of low sunlight [27].

The efficiency of solar power production systems depends on several factors, including the amount of sunlight available, the temperature, and the efficiency of the solar panels. The efficiency of solar panels has improved significantly in recent years, with some panels now capable of converting over 20% of the sunlight they receive into electricity [16]. This has made solar power production more cost-effective and attractive to homeowners and businesses [14].

One of the most significant advantages of solar power production is its environmental benefits. Solar power produces no greenhouse gas emissions or other pollutants, making it a clean and sustainable energy source [18]. This can help reduce our dependence on fossil fuels and mitigate the impacts of climate change [13, 28].

In addition to its environmental benefits, solar power production can also provide economic benefits. Installing solar panels on homes and businesses can help reduce electricity bills and provide a reliable energy source. In some cases, excess energy generated by solar panels can be sold back to the grid, providing additional income for homeowners and businesses [29].

However, there are also some challenges associated with solar power production. One of the biggest challenges is the intermittency of sunlight, making it difficult to rely on solar power as a primary energy source [23]. This can be addressed through batteries or other energy storage systems, which can store excess energy generated during the day for use at night or during periods of low sunlight [30].

Another challenge is the initial cost of installing solar panels, which can be significant. However, the cost of solar panels has decreased significantly in recent years, making solar power production more accessible to homeowners and businesses [16, 29].

Despite these challenges, solar power production has the potential to play an essential role in our transition to a more sustainable energy future. As the technology continues to improve and the cost of solar panels continues to decrease, we can expect to see increased adoption of solar power production in homes, businesses, and industries worldwide.

2.1.3 Wind Power

Wind power production is the process of generating electrical power using the wind's kinetic energy. It is a form of renewable energy that has become increasingly popular in recent years due to its low environmental impact and economic benefits [18]. Wind power can be generated using various methods, including wind turbines, wind farms, and offshore wind farms.

Wind turbines are the most common method of generating wind power. They consist of a rotor, blades, a gearbox, a generator, and a tower. The rotor and blades capture the wind's kinetic energy and convert it into mechanical energy. This mechanical energy is then transferred to the gearbox, which increases the rotational speed of the generator. The generator converts this mechanical energy into electrical energy, which is sent to a power grid or stored in batteries [31].

Wind turbines can be located on land or offshore. On land, they are typically installed in areas with high wind speeds, such as hills, ridges, or open plains. Offshore wind turbines are located in shallow water near the coast or deep offshore waters. Offshore wind farms can generate more power than onshore wind farms due to the stronger and more consistent winds found at sea [32].

Wind farms are collections of wind turbines installed together to generate large amounts of electricity. They can be located on land or offshore and range in size from a few turbines to hundreds. Wind farms are typically connected to a power grid that distributes electricity to homes and businesses.

Offshore wind farms have become increasingly popular in recent years due to their potential to generate large amounts of electricity. Offshore wind farms are typically located in areas with deep water, strong winds, and a shallow continental shelf. They can be more expensive to build than onshore wind farms, but they can generate more electricity and have a lower environmental impact [32].

Wind power has several advantages over other forms of energy. It is a clean and renewable energy source that produces no greenhouse gases or air pollution. Wind power also impacts wildlife less than other forms of energy, such as fossil fuels or hydroelectric power [18]. Wind turbines can be installed on land used for farming or other purposes, providing additional income to landowners [29].

Despite its many advantages, wind power also has some disadvantages. Wind turbines can be noisy, which can be a problem for people living nearby. Wind turbines can also harm birds and bats, which can collide with the blades. The construction of wind turbines can also

damage the environment, particularly if they are located in sensitive areas such as wetlands or forests [18]. A major disadvantage of wind power production is its intermittency and the need for a balancing component for stable power production.

The amount of electricity generated by wind power depends on several factors, including wind speed, wind direction, and the size and efficiency of the wind turbine. Wind power is most effective in areas with consistent and strong winds, such as coastal regions and high-altitude areas [31].

The efficiency of wind turbines has improved significantly in recent years. Modern wind turbines can generate electricity at a lower cost than traditional fossil fuel power plants in some regions. The cost of wind power has also decreased significantly in recent years due to technological improvements and economies of scale [16].

2.2 Electrical Transmission and Distribution

The typical European electrical power grid configuration comprises a high-voltage transmission system and a lower-voltage distribution system that delivers electric power to end users. The structure varies somewhat from country to country, but the general principles are similar [17].

At the heart of the Norwegian power grid is a network of high-voltage transmission lines that span the country. These lines carry power from large power plants, wind farms, and other generation sources to regional substations. The transmission lines are typically operated at voltages from 132kV to 420 kV, depending on the specific transmission system [33, 34].

At the regional substations, the voltage is stepped down to an intermediate level, typically 66 kV or 132 kV, before it is sent out on the distribution network. The distribution network consists of a network of lower-voltage lines, normally operating at 22 kV or 11 kV, delivering power to end users [17].

The distribution network is typically divided into primary and secondary networks. The primary network consists of more extensive distribution lines that deliver power to substations in urban areas. In comparison, the secondary network consists of smaller lines that provide power to individual homes and businesses [35].

The transmission and distribution system plays a critical role in the overall reliability and efficiency of the electric power system. Efficient transmission systems ensure electric power is transported from the generating stations to the end users with minimal losses. Energy losses during transmission can result from various factors, such as resistance in the transmission lines, reactive power losses, and thermal losses [36]. System operators use advanced monitoring and control systems to optimize power flow and minimize losses, ensuring that electric power is delivered reliably and efficiently.

The power grid is operated and managed by transmission system operators (TSOs) and distribution system operators (DSOs). TSOs are responsible for operating the high-voltage transmission network, while DSOs are responsible for operating the distribution network [33].

To ensure the stability and reliability of the power grid, TSOs and DSOs use sophisticated control systems and monitoring equipment to manage the power flow and maintain the

balance between supply and demand. These systems allow operators to detect and respond to issues in real-time, such as power outages, overloads, and voltage fluctuations [37].

The European power grid is also interconnected with neighboring countries through a system of cross-border transmission lines. These interconnections allow power to be shared across borders, which helps to balance supply and demand and maintain system stability [38].

The design, operation, and maintenance of electrical transmission and distribution systems require expertise in various engineering disciplines, including electrical, mechanical, civil, and environmental engineering. When designing and operating distribution systems, system engineers must consider load demand, voltage regulation, distribution line routing, environmental impact, and regulatory compliance.

There has been a growing emphasis on developing smart grid technologies and renewable energy sources in Norway in recent years. Smart grid technologies such as advanced metering systems, automated control systems, and demand response programs can enhance the power grid's reliability, efficiency, and sustainability [3, 36, 39].

2.2.1 Smart grids

An electrical smart grid is a modern power distribution system that utilizes advanced communication, control, and computing technologies to optimize power generation, distribution, and consumption. Smart grids enable real-time monitoring and control of energy usage through two-way communication between utilities and customers [39].

Smart grids incorporate advanced metering infrastructure to provide detailed information about energy usage. This information can be utilized to develop pricing models that encourage customers to use power during off-peak hours, reducing overall demand on the grid. Additionally, smart grids integrate distributed energy resources, such as rooftop solar panels and small-scale wind turbines, and energy storage technologies to store excess energy and reduce the need for additional generation and distribution capacity [40].

Smart grids use predictive analytics to forecast energy demand and optimize power generation and distribution. This helps utilities anticipate and mitigate potential problems before they occur, reducing the likelihood of power outages and other disruptions [41].

The benefits of smart grids are numerous. By providing more detailed information about energy usage, smart grids enable consumers to make more informed decisions about their energy consumption, which can help them save money on their energy bills. Smart grids also help reduce the overall grid demand, which can lower the need for new power generation and distribution infrastructure and reduce greenhouse gas emissions [29].

For utilities, smart grids provide more detailed and accurate information about the state of the power grid, which helps them manage the grid and reduce the likelihood of power outages more efficiently. Smart grids also enable utilities to effectively integrate renewable energy sources, such as solar and wind power, into the grid, reducing reliance on fossil fuels and making the grid more sustainable in the long term [17, 40].

2.2.2 Electrical grid island operation

Power grid island operation refers to the ability of a power system to operate in a self-contained manner when disconnected from the main grid. In other words, when a part of the power system is isolated from the rest of the grid due to a fault or other disturbances, it can continue to generate, transmit, and distribute electricity using its own resources [42].

The primary goal of power grid island operation is to ensure the continuity of power supply to critical loads such as hospitals, emergency services, and other vital infrastructure during a power outage or system disturbance [43]. It is especially important for isolated areas or regions not connected to the main grid, as it allows them to continue operating even if there is a disruption in the main power supply [44]. To maintain island operation, a power system must have sufficient generation capacity, transmission and distribution infrastructure, and control systems to manage the supply and demand of electricity within the island. This requires careful planning and design of the power system and the implementation of advanced control and monitoring technologies to ensure that the island operates stably and securely[42].

The success of power grid island operation depends on the ability of the power system to maintain a balance between the generation and consumption of electricity within the island [43]. This requires sophisticated control algorithms and advanced monitoring systems to continuously adjust the output of generators and manage the flow of electricity in the system [44].

One of the critical challenges of power grid island operation is the need for a reliable and secure power source. This can be achieved through backup generators, energy storage systems, or the integration of renewable energy sources such as solar or wind power [17]. In addition, a robust communication and control infrastructure is essential to ensure that the power system can be operated safely and securely during island operation [44].

Overall, power grid island operation is an important aspect of power system design and operation. It ensures the reliability and continuity of power supply in isolated regions or during system disturbances. It requires careful planning, design, and implementation of advanced control and monitoring technologies to ensure that the island operates stably and securely.

2.3 Electrical Energy Storage

Electrical energy storage can in large be categorized into two sections in the industrial market. One category is electrochemical battery storage, and the other is mechanical energy storage. Both categories have strengths and weaknesses, where battery storage has a short reaction time and high energy density but low power capacity while mechanical storage has higher energy capacity and power density but a longer reaction time and higher cost. Both categories are instrumental when operating an energy system with high VRE penetration.

2.3.1 Battery storage

Electricity grid battery storage is a technology that has been gaining increasing attention in recent years to address the challenges posed by integrating renewable energy sources into the electricity grid [16, 44]. It involves using batteries to store excess electricity generated by renewable sources, such as wind and solar power, and release it when needed to meet

demand. The use of battery storage in the electricity grid can improve grid reliability, increase the penetration of renewable energy sources, and reduce greenhouse gas emissions [18, 27].

One of the challenges of the electricity grid is that electricity must be generated and consumed in real-time, which means that the electricity supply must always be balanced with the demand [17]. Traditionally, this has been achieved by adjusting the output of power plants to match changes in the demand [12]. However, integrating renewable energy sources, such as wind and solar power, has made it more challenging to balance the grid, as these sources are intermittent and can fluctuate rapidly [16].

Electricity grid battery storage solves this challenge by allowing excess electricity generated by renewable energy sources to be stored and released when needed [27]. Battery storage systems can be used to smooth out the variability of renewable energy sources, providing a more stable and reliable source of electricity. This can help to reduce the need for conventional power plants and improve the efficiency of the electricity grid [44].

Several different types of battery storage systems can be used on the electricity grid. One of the most common types is lithium-ion batteries, widely used in consumer electronics and electric vehicles [27]. Lithium-ion batteries have a high energy density, which means they can store a large amount of electricity in a small space. They are also relatively efficient and can be charged and discharged quickly [45]. Other types of batteries that can be used for electricity grid storage include lead-acid batteries, flow batteries, and sodium-sulfur batteries [46].

A large-scale electrical battery is a device that stores electrical energy in chemical form and then converts it back into electrical energy when needed. The battery consists of several modules, each of which contains a number of cells. The cells are connected in series and parallel to form a battery pack.

Each cell consists of a positive electrode (cathode), a negative electrode (anode), and an electrolyte. The electrodes are typically made of a metal oxide (such as lithium cobalt oxide or nickel cobalt aluminum oxide) and graphite, respectively. The electrolyte is a liquid or gel that allows the flow of ions between the electrodes [45, 46].

When the battery is charged, electrical energy is stored in the cells by transferring lithium ions from the cathode to the anode through the electrolyte. When the battery is discharged, the process is reversed, and the lithium ions flow from the anode back to the cathode, producing an electrical current.

Battery storage can provide several economic benefits [29, 47]. For example, it can help to reduce the need for expensive peak power plants, which are only used during periods of high demand. Battery storage can also help to reduce transmission and distribution costs by reducing the need for new transmission lines and other infrastructure [17]. In addition, battery storage can provide a new revenue stream for utilities by allowing them to sell excess electricity back to the grid when demand is high [38, 48].

Despite the many benefits of electricity grid battery storage, some challenges must be addressed. One of the main challenges is the cost of battery storage systems. While the cost of batteries has been declining rapidly in recent years, they still represent a significant investment [29, 49]. In addition, battery storage systems require regular maintenance and replacement of batteries, which can add to the overall cost [27, 45].

Another challenge is the technical limitations of battery storage systems. While batteries can provide backup power and help to smooth out fluctuations in demand, they cannot offer long-term storage over several days or weeks. This means other forms of energy storage are needed [14].

2.3.2 Mechanical storage

The most used types of mechanical energy storage in electricity grids include pumped hydroelectric storage, compressed air energy storage, flywheel energy storage, gravitational potential energy storage, and advanced rail energy storage [49]. Compressed air energy storage involves compressing air and storing it underground, releasing and expanding it through turbines to generate electricity when needed. Flywheel energy storage stores energy in the form of rotational kinetic energy and converts it to electricity using a spinning rotor connected to a generator. Gravitational potential energy storage lifts heavy objects or uses weights to store and release potential energy for electricity generation. Advanced rail energy storage uses rail systems to move loaded railcars uphill with excess electricity and release them downhill to generate electricity [47, 49, 50]. Pumped hydroelectric storage is the most prevalent and mature technology. Pumped hydro is also the mechanical storage technology with the most potential in Norway and will therefore be the focus further in this thesis [19, 51].

Hydroelectric energy storage is a technology that uses water reservoirs to store energy in the form of potential energy. It is a well-established technology that has been used for many years to provide backup power and stabilize the electricity grid [19]. Hydroelectric energy storage is an essential technology for meeting the challenges posed by integrating renewable energy sources into the electricity grid. It can store excess electricity from renewable sources, such as wind and solar power [14, 44].

Hydroelectric energy storage works by pumping water from a lower reservoir to an upper reservoir during periods of low electricity demand, using excess electricity generated by renewable sources [51]. The potential energy stored in the upper reservoir is then released when electricity demand is high by allowing the water to flow back to the lower reservoir, driving turbines and generating electricity. The energy stored in the upper reservoir can be used to provide backup power in the event of a power outage or to smooth out fluctuations in demand, helping to stabilize the electricity grid [52].

Hydroelectric energy storage systems can store large amounts of energy for long periods, making it a suitable technology for meeting the challenges posed by integrating renewable energy sources into the electricity grid [50]. Hydroelectric energy storage can help address intermittency by storing excess electricity generated by renewable sources, such as wind and solar power, and releasing it when needed [52].

Another benefit of hydroelectric energy storage is that it can provide a reliable backup power source. In the event of a power outage or other grid disturbance, the stored energy in the upper reservoir can be released to provide backup power, helping to maintain grid stability and reliability. Hydroelectric energy storage can also provide emergency power during natural disasters or other emergencies, helping ensure that critical infrastructure remains operational [18].

Hydroelectric energy storage can also provide several environmental benefits. Hydroelectric energy storage systems do not emit greenhouse gases or other pollutants, making them a clean and sustainable energy source. In addition, hydroelectric energy storage can help reduce the need for conventional power plants, which can be a significant source of greenhouse gas emissions [14].

Despite the many benefits of hydroelectric energy storage, some challenges must be addressed. One of the main challenges is the high cost of building and maintaining hydroelectric energy storage systems. Hydroelectric energy storage systems require constructing large reservoirs and installing turbines and other equipment, which can be expensive [29, 47]. In addition, hydroelectric energy storage systems require regular maintenance and upkeep, which can add to the overall cost [53].

Another challenge is the limited availability of suitable sites for hydroelectric energy storage. Hydroelectric energy storage requires the availability of two large reservoirs, one upper and one lower, with a significant elevation difference. Finding suitable sites for hydroelectric energy storage can be challenging, particularly in densely populated areas[47, 51, 52].

2.4 Mathematical Modeling

Mathematical optimization is a field of study that covers finding the best possible solution to a given problem, subject to certain constraints. It involves using mathematical techniques to determine the optimal values of decision variables, which can lead to an objective function's maximum or minimum value [41].

One of the most common types of mathematical optimization is linear programming, which involves optimizing a linear objective function subject to a set of linear constraints. In linear programming, the objective function is a linear combination of the decision variables, and linear equations or inequalities represent the constraints. The solution to a linear programming problem is a set of values for the decision variables that maximize or minimize the objective function, subject to the constraints [54].

Another type of mathematical optimization is nonlinear programming, which involves optimizing a nonlinear objective function subject to a set of nonlinear constraints. Nonlinear programming problems are more complex than linear programming problems, and the solution to such problems is usually found using iterative algorithms that use calculus and numerical optimization techniques [55].

In addition to linear and nonlinear programming, there are other types of mathematical optimization, such as integer programming, which involves optimizing an objective function subject to the constraint that the decision variables are integers, and mixed-integer programming, which consists in optimizing an objective function subject to the constraint that some of the decision variables are integers while others are continuous [41].

One of the main challenges in mathematical optimization is the complexity of the problems, which often involve a large number of decision variables and constraints. As a result, solving optimization problems requires efficient algorithms that can handle large-scale problems. Fortunately, advances in computer technology have led to the development of powerful optimization software that can solve complex problems efficiently [30, 56-58].

In recent years, there has been increasing interest in using machine learning techniques for optimization. Machine learning algorithms can learn the structure of complex optimization problems and guide the search for optimal solutions. For example, reinforcement learning algorithms can be used to discover the optimal policies for decision-making problems in dynamic environments [44, 59, 60].

In addition to machine learning, other advanced techniques such as stochastic optimization, game theory, and multi-objective optimization are being developed to address more complex optimization problems. Stochastic optimization involves optimizing an objective function subject to uncertain or random parameters, while game theory involves optimizing the decisions of multiple agents with conflicting objectives. Multi-objective optimization involves optimizing multiple conflicting objectives simultaneously and finding the set of solutions that are optimal with respect to all objectives [41].

2.4.1 MILP

Mixed integer linear programming (MILP) is a type of mathematical optimization that involves optimizing a linear objective function subject to a set of linear constraints, where some decision variables are required to take integer values. MILP is a generalization of linear programming, allowing continuous and integer variables [30, 58].

In MILP, the decision variables are divided into two sets: continuous variables that can take any value within a given range and integer variables that are restricted to taking integer values. The objective function and the constraints are linear functions of both the continuous and integer variables [41].

The solution to a MILP problem is a set of values for the decision variables that satisfies all of the constraints and maximizes or minimizes the objective function. However, solving MILP problems can be challenging due to integer variables, which make the problem non-convex and non-linear. As a result, MILP problems require specialized algorithms that can handle the integer variables and ensure that the solution is optimal [54].

Several techniques are used to solve MILP problems, including branch and bound, branch and cut, and integer programming relaxations. Branch and bound is a general-purpose algorithm that systematically partitions the feasible region of the problem into smaller subproblems until the optimal solution is found. Branch and cut is a similar algorithm that combines branch and bound with additional constraints called cuts, which help to eliminate infeasible solutions [41]. Integer programming relaxations involve solving a relaxed version of the MILP problem, where the integer variables can take on fractional values. The solution to the relaxed problem can provide helpful information about the optimal solution to the original MILP problem [54].

2.4.2 Prescriptive analytics

Prescriptive analytics is a type of data analytics that focuses on using advanced mathematical and computational methods to recommend the best course of action for a given situation. Prescriptive analytics goes beyond descriptive and predictive analytics by identifying what

happened in the past or what might happen in the future and providing a recommended action to achieve a desired outcome [60, 61].

Prescriptive analytics involves using optimization algorithms, simulation models, and decision analysis techniques to evaluate multiple scenarios and recommend the best course of action based on predefined criteria or objectives [62]. Prescriptive analytics aims to help decision-makers make more informed and effective decisions by providing them with actionable insights based on data and analytics [63].

One of the key benefits of prescriptive analytics is that it can help organizations make more objective and data-driven decisions. By providing decision-makers with recommendations based on data and analytics, prescriptive analytics can help to reduce bias and subjectivity in the decision-making [62]. Additionally, prescriptive analytics can help organizations identify opportunities for optimization and improvement, leading to increased efficiency and cost savings [54].

Organizations need access to high-quality data, advanced analytics tools, and skilled data scientists or analysts to implement prescriptive analytics. Implementing prescriptive analytics involves several steps, including data collection, data cleaning and preparation, model development and validation, and deployment [41].

3 Method & Data

3.1 Area

3.1.1 Area selection

Located along Norway's coastline at approximately 69° north, Senja is the country's second-largest island, spanning an area of 1,589.35 km2. The island's mountainous landscape features numerous fjords and valleys, resulting in a multitude of distinct, small communities scattered across the island. With a population of roughly 14,000 inhabitants, many rely on the fishing and seafood industries, while others depend on the growing tourism sector [64]. This thesis will primarily focus on parts of the island afflicted by increasing demand and electricity limitations in the distribution network. As such, these locations are frequently associated with challenges related to voltage drops stemming from the extended distance of power lines in the distribution network.

This thesis aligns with the "Transformation to a Renewable & Smart Rural Power System Community RENEW" project, a collaboration between ARC (The Arctic Centre of Sustainable Energy) - an interdisciplinary center affiliated with UiT, Norway's Arctic University - and Troms Kraft, a local power company. Also related is the "Smart Senja" project, an internal initiative by Troms Kraft that also evaluates innovative solutions to address the power network's limitations. Both projects aim to find solutions to Senja's network issues, as the community's aging power distribution network is nearing its capacity amidst increasing demand for power. The projects consider methods such as power flow control, cooperation agreements with customers for regulated power purchase, use of batteries, and cooperation agreements with local power producers. The thesis originates from the consideration of alternative solutions for local power production and storage while also researching the possibility of island operation of the local distribution grid. Locations of interest within the area are selected on the basis of future increase in electricity demand reported by consumers and producers [4, 65, 66].

3.1.2 Network radials

The distribution network of Senja is divided into a multitude of radials running from central transformer stations to remote villages and fjords with small communities. These radials proved a useful way to separate the distribution network into nodes as most of them end up in locations with high electricity consumption, as seen in Figure 3-1 and Figure 3-2. The separation of radials is shown in Table 3-1.

Table 3-1 Distribution network radials.

Name	Zone	# connected network stations	Origin	Destination
SILS 22GI1	Z1	82	Silsand	Botnhamn

STRA 22O1	Z2	70	Straumsnes	Torsken
SVAN 22SI1	Z3	69	Svanelvmoen	Rubbestad
SVAN 22LY1	Z4	69	Svanelvmoen	Husøy
STRA 22SV1	Z5	56	Straumsnes	Senjahopen
STON 22OS1	Z6	51	Stonglandseidet	Flakstadvåg
STRA 22SK1	Z7	46	Straumsnes	Senjahopen
SVAN 22SS1	Z8	35	Svanelvmoen	Tranøy
STON 22ST1	Z9	24	Stonglandseidet	Sjurvika
SILS 22SV1	Z10	24	Silsand	Silsand
YTTRE (145KV)	Z11		Bardufoss	Finnfjordbotn
SILS (66KV)	Z12		Finnfjordbotn	Silsand
STRA (66KV)	Z13		Svanelvmoen	Straumsnes
STON (66KV)	Z14		Svanelvmoen	Stonglandseidet
SVAN (66KV)	Z15		Silsand	Svanelvmoen
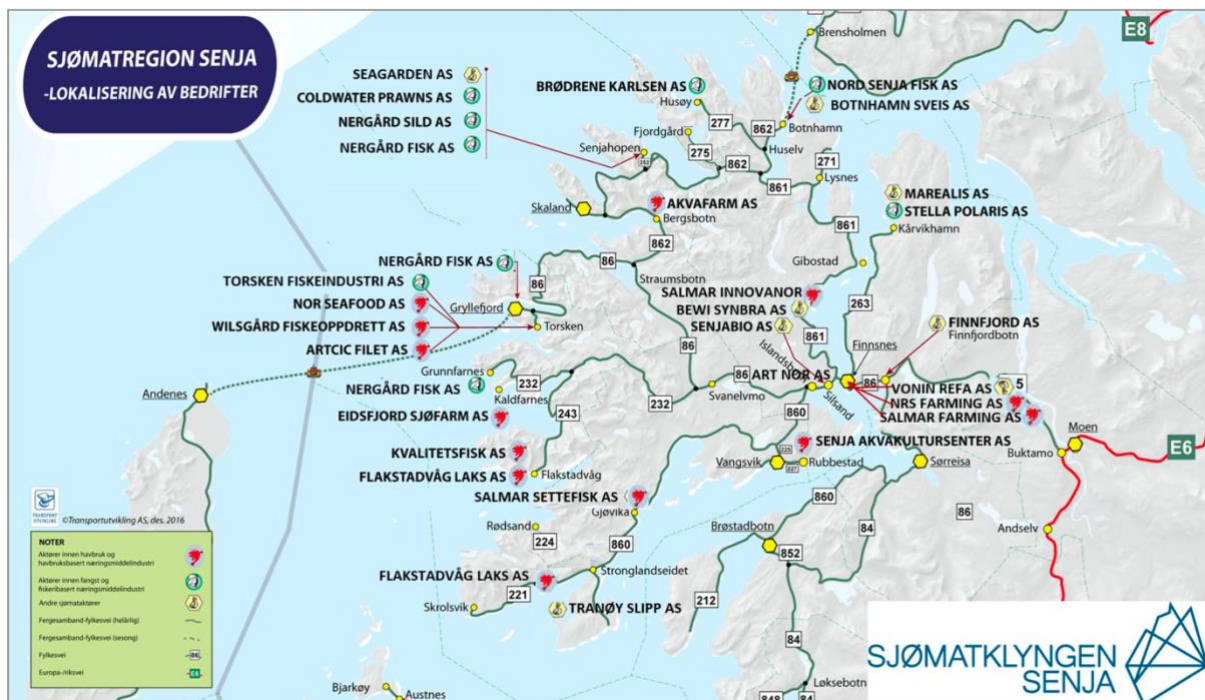
Figure 3-1 Location of seafood facilities on Senja [Sjømatklyngen Senja].

3.1.3 Existing hydropower

The three hydroelectric power plants installed on Senja are all in the category of small power plants with a capacity between 1MW and 9.999MW. All of them are owned by Tromskraft Produksjon, a daughter company of Tromskraft, and built in the 20th century. Technical specifications of these power plants are presented in Table 3-2 and the geographical location of the power plants is shown in Figure 3-2 [67].

Table 3-2 Hydroelectric power plants located within the modeling area today.

Name	Power [MW]	Power [MVA]	Production [GWh]	Capacity [GWh]	Head [m]
Bergsbotn	8.5	10	26.1	21.1	350
Lysbotn	5.35	6.3	28	8.45	108
Osteren	2.52	3.15	13.7	2.56	134.5
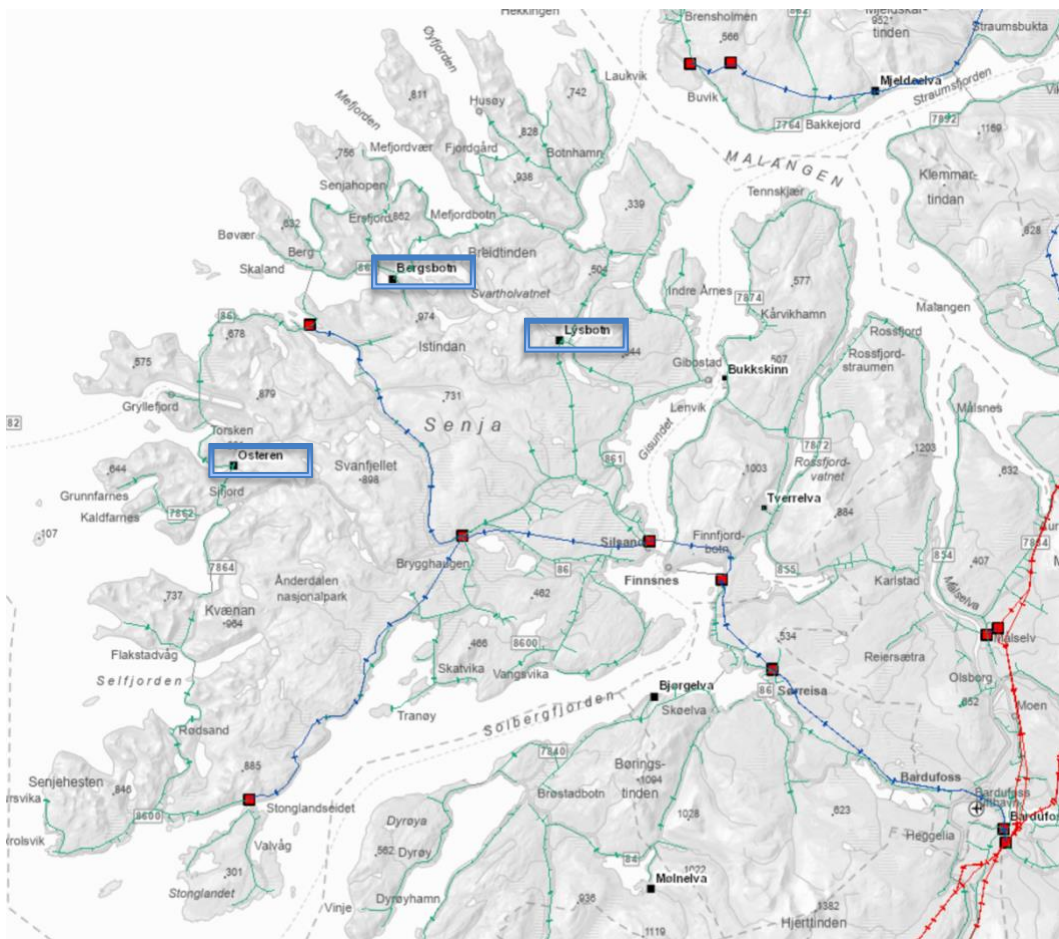
Figure 3-2 Local hydroelectric generators are marked as black squares highlighted with blue squares [atlas.nve.no].

These three power plants have shown very important for the power quality and voltage control along the powerlines in the outermost parts of Senja. Adding voltage between the central transformer stations and the consumption at the end of radials can be seen as a form of series compensation keeping the voltage stable over longer distances [3, 12].

3.2 Model Building

The chosen tool for model building in this study is a free modeling code package called GenX. GenX is an open-source model that enhances the capacity of electricity resources by incorporating advanced techniques for electricity system planning. Its primary objective is to provide improved decision support in the ever-changing landscape of the power sector.

Operating as a constrained linear or mixed integer linear optimization model, GenX determines the optimal mix of investments and operational choices for various components, including demand-side resources, storage, transmission, and electricity generation. Its goal is to minimize costs while adhering to environmental regulations, market requirements, and policy constraints. The model considers one or more future planning years, ensuring efficient electricity supply to meet demand [68].

Built using Julia + JuMP, GenX boasts a transparent and modular code structure. This design allows for maximum flexibility and adaptability, enabling its utilization in diverse applications such as academic research, technological assessments, public policy analysis, regulatory evaluations, and resource planning [69]. Depending on the specific planning problem or research question, the model can be tailored to different levels of resolution and scope in terms of temporal, operational, and geographical considerations.

GenX includes a comprehensive range of electricity sources, encompassing both traditional and cutting-edge technologies. It can represent thermal generators, variable renewable energy sources like wind and solar, run-of-river and hydroelectric generators, energy storage systems, demand-side flexibility, demand response, and emerging solutions like long-duration energy storage. By encompassing these elements, GenX provides a comprehensive framework for analyzing and optimizing the electricity system.

3.2.1 Distribution infrastructure

Transformers in GenX

A transformer is an electrical machine with the ability to change the voltage of a transmission or distribution line with a set frequency to another voltage level with the same frequency [12]. The size and capacity of a transformer can vary largely from millivolts to megavolts. In the Norwegian electrical grid, there are transformers in the range of 230 Volts to 420 Kilovolts. One great advantage of modern transformers is the high efficiency of the machines, working with below 1% loss at rated conditions [17].

The basic construction of an ideal transformer has two coils wrapped around a magnetic core. In the modern power grid, the main bulk of transformers is three-phase transformers with six coils in three coil pairs wrapped around a mutual core. Each coil pair is divided into a primary and secondary coil, where the primary coil usually is the one with a higher voltage. A model of a three-phase transformer is seen in Figure 3-3 displaying the four major imperfections of a modern transformer with p- and s-subscripts annotating the primary and secondary side. The

four major imperfections of a transformer are copper losses (R), eddy current losses (X), hysteresis losses (R_c), and leakage flux (jX_m) [12].
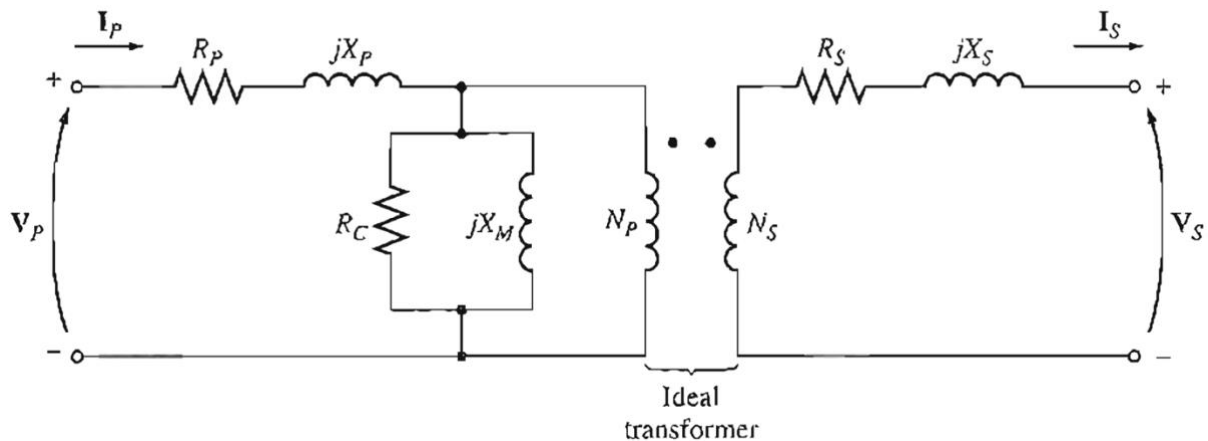
Figure 3-3 Realistic model of a transformer, with its largest loss contributes [Chapman,2012].

In the Senja grid, there are four large transformers connected to the regional network seen in Figure 3-2 as red squares, with a plethora of smaller transformers in the distribution network. These smaller transformers are called network stations. Within the confinements of this thesis, large transformer stations are regarded as lossless connection nodes connected to the rigid regional network. Losses from these transformers are small enough to be neglected as they represent a fraction of a decimal percentage of the overall power in the network.

Network stations in GenX

Network stations are small transformers in the distribution network. The main task of these machines is to bring the voltage from distribution voltage, usually at 22 kilovolts, down to 400 volts or 230 volts. The secondary winding voltage depends on the connection used at the secondary side. If the low voltage side is a NT-system the voltage is brought down to 400 volts, and if it is an IT-system the terminal voltage is 230 volts. Network stations also contain overvoltage protection, circuit breakers, disconnectors, current and voltage measurements, and earth connections [17]. For modeling purposes, the network stations are used as distributed data collection points within the distribution network at Senja. As network stations always measure the connected load, they are ideal for collecting the data needed for the model.

Power lines in GenX

Power lines in Norway refer to the infrastructure used to transmit electricity from power plants to distribution centers and end-users. These power lines form the backbone of the electricity grid that powers homes, businesses, and industries throughout the country. Power lines are divided into different categories based on voltage and power capacity. On Senja the electrical grid is separated into four distinct subsets with the 132kV external transmission grid, the 66kV regional grid, the primary distribution grid of 22kV, and the secondary distribution grid of 400V or 230V. Transmission lines are managed by the Transmission System Operator (NVE) who oversees the transmission of electricity within the nation and

across national borders [17]. Distribution lines are managed by the Distribution System Operator (ARVA) who maintains and operates the local distribution networks [17]. Smart grids are an advanced form of electricity grid that uses digital technologies to monitor and control the flow of electricity. This type of grid is implemented on Senja as a part of the Smart Senja project. Smart grids can help to improve energy efficiency, reduce costs, and enable the integration of renewable energy sources such as wind and PV [43]. Included in the model smart grids can reduce load when needed and operate VRE optimally through curtailment. In the model, electrical transmission and distribution is calculated as constraints shown in Equation (3-1).

$$-\varphi_l^{max} \leq \Phi_{(l,t)} \leq \varphi_l^{max} \, , \forall \, l \in (\boldsymbol{L}\backslash\boldsymbol{E}), \forall \, t \in \boldsymbol{T}$$

$$-(\varphi_l^{max} + \Delta\varphi_l^{max}) \leq \Phi_{(l,t)} \leq (\varphi_l^{max} + \Delta\varphi_l^{max}) \, , \forall \, l \in \boldsymbol{E}, \forall \, t \in \boldsymbol{T}$$

$$\Delta\varphi_l^{max} \leq \overline{\Delta\varphi_l^{max}} \, , \forall \, l \in \boldsymbol{E}$$

$$(\, 3\text{-}1 \,)$$

Where φ_l^{max} denotes maximum power transfer capacity, $\Phi_{l,t}$ denotes power flow, and $\Delta\varphi_l^{max}$ is the maximal added power transfer capacity. Subscript l denotes line segment and t denotes timestep.

Generators in GenX

An electrical machine is defined as a machine that can produce electrical power from mechanical work, or vice versa [12]. A synchronous generator is a type of electrical generator that produces AC by converting mechanical energy into electrical energy. It is called "synchronous" because its output frequency is synchronized with the rotation speed of the generator's rotor. Synchronous generators are widely used in power plants, renewable energy systems, and industrial applications where reliable and efficient power generation is required. The construction of a synchronous generator consists of two major components: the rotor and the stator. The rotor is the rotating part of the generator that houses the field winding, which generates the magnetic field necessary for power generation. The stator is the stationary part of the generator that houses the armature winding, which produces the electrical output. The rotor and stator are separated by an air gap to prevent electrical short circuits [70].

The field winding of the rotor is typically excited by a DC source, which creates a magnetic field that rotates with the rotor. The armature winding of the stator is connected to the load, which draws electrical power from the generator. When the rotor rotates, the magnetic field induces an alternating voltage in the armature winding, which generates AC power.

The output frequency of a synchronous generator is determined by the speed of the rotor and the number of poles in the field winding. The number of poles in the field winding is determined by the design of the generator and can range from two to several dozen. The higher the number of poles, the lower the rotational speed required to achieve a given output frequency [12].

Most large generators in the Norwegian electrical network are synchronous generators connected at the same frequency [33]. There are other types of generators in the electrical energy mix, such as induction generators and DC-generators connected via alternators and

other power electronics. These machines are not frequency connected and do not contribute to much, other than active power. For other purposes such as reactive power control and frequency regulation, a synchronous generator is preferred.

In the model, generators are represented within the nodes as power sources. As some of the generators already installed in Senja are not geographically located within each node some loss is added depending on the distance from each node according to Equation (3-2).

$$P_l = 3 \cdot I_l \cdot X_l^2 \cdot R$$

Here P_l denotes the power loss in the line segment, I_l is the line current, X_l^2 denotes the line reactance, and R is the resistance.

When modeling for the addition of new local production no loss is added as the new sources are meant to be built in immediate proximity to each node. Generators are together with energy storage, used to maintain power balance in the network, calculated through Equation (3-3).

$$\sum_{y \in W} \Phi_{y,z,t} + \sum_{y \in vre} \Phi_{y,z,t} + \sum_{y \in O} (\Phi_{y,z,t} - \Pi_{y,z,t}) + \sum_{s \in S} \Lambda_{s,z,t} - \sum_{l \in L} (\varphi_{l,z} \times \Phi_{l,t})$$
$$- \frac{1}{2} \sum_{l \in L} \left(\varphi_{l,z}^{map} \times \beta_{l,t}(\cdot) \right) = D_{z,t} , \forall z \in Z, t \in T$$

As shown in the constraint, electricity demand $D_{z,t}$ at each time step and for each zone must be strictly equal to the sum of generation $\Theta_{y,z,t}$ curtailable VRE resources, and hydro resources (W). At the same time, energy storage devices (O) can discharge energy $\Theta_{y,z,t}$ to help satisfy demand, while when these devices are charging $\Pi_{y,z,t}$ they increase demand. Price-responsive demand curtailment $\Lambda_{s,z,t}$ reduces demand. Finally, power flows $\Phi_{l,t}$ on each line into or out of a zone (defined by the network map $\varphi_{l,z}^{map}$), are considered in the demand balance equation for each zone. In the subscripts, y denotes different resources, z denotes zones, t denotes timesteps, and l denotes line segments.

Electrical storage batteries in GenX

Batteries can be used for multiple purposes, with the most common being load-shedding and voltage control. When installing a battery for a specific task, it is important to match the connection configuration for that task. Load-shedding and long-time storage require large-capacity batteries with small trickle losses. Voltage regulation batteries do not require the same capacity but must be able to react fast with high power outputs.

Large-scale electrical batteries typically have a capacity of several megawatt-hours (MWh) and are designed for long-duration storage. They are often used in conjunction with renewable energy sources, such as wind or solar power, to store excess energy and then release it when needed. They are also used for grid stabilization, providing frequency regulation and voltage support.

In addition to the cells and modules, a large-scale electrical battery also includes a battery management system (BMS) that monitors the battery's state of charge, temperature, and other parameters to ensure safe and efficient operation. The BMS also controls the charging and discharging of the battery to optimize its performance and lifespan [45].

In the model, batteries are represented as energy storage within each node with no associated transfer loss. Batteries include operational losses both for charge and discharge, in addition to leakage loss for storage over longer time periods. In the baseline scenario, two batteries will be installed. One of the batteries is located in Senjahopen, and the other on Husøy.

Electrical storage can be implemented in multiple ways in the model. For this thesis, a generic formulation of symmetric charge and discharge has been chosen as this will cover the technologies of interest. For storage with symmetric charge and discharge capacity, operation is regulated through two constraints, shown in Equation (3-4) and Equation (3-5). With $\Pi_{o,z,t}$ and $\Phi_{o,z,t}$ denoting charge rate and discharge rate, respectively, $f_{o,z,t}^{charge}$ and $f_{o,z,t}^{discharge}$ denoting contribution to frequency regulation for charging and discharging, respectively, and $\Delta_{o,z}^{total}$ is the total installed power capacity. Further, the state of charge is regulated according to the volume of energy stored confined by the constraints in Equation (3-6) and Equation (3-7). Here $\Gamma_{o,z,t}$ denotes the volume of energy stored, $\eta_{o,z}^{charge}$ denotes the charge/discharge efficiency, and $\eta_{o,z}^{loss}$ is the self-discharge rate (if any). The first of these controls the initial time step, and the latter handles the interior time steps. As for subscripts, o denotes storage unit, z denotes zone, and t denotes timestep.

$$\Pi_{o,z,t} + f_{o,z,t}^{charge} \leq \Delta_{o,z}^{total} \ , \forall \ o \in \boldsymbol{O}^{sym} \ , z \in \boldsymbol{Z} \ , t \in \boldsymbol{T}$$

(3-4)

$$\Pi_{o,z,t} + f_{o,z,t}^{charge} + \Phi_{o,z,t} + f_{o,z,t}^{discharge} + r_{o,z,t}^{discharge} \leq \Delta_{o,z}^{total} \ , \forall \ o \in \boldsymbol{O}^{sym} \ , z \in \boldsymbol{Z} \ , t \in \boldsymbol{T}$$

(3-5)

$$\Gamma_{o,z,t} = \Gamma_{o,z,t+\tau^{period}-1} - \frac{1}{\eta_{o,z}^{discharge}} \Phi_{o,z,t} + \eta_{o,z}^{charge} \Pi_{o,z,t} - \eta_{o,z}^{loss} \Gamma_{o,z,t+\tau^{period}-1} \ , \forall \ o \in \boldsymbol{O} \ , z \in \boldsymbol{Z} \ , t \in \boldsymbol{T}^{start}$$

(3-6)

$$\Gamma_{o,z,t} = \Gamma_{o,z,t-1} - \frac{1}{\eta_{o,z}^{discharge}} \Phi_{o,z,t} + \eta_{o,z}^{charge} \Pi_{o,z,t} - \eta_{o,z}^{loss} \Gamma_{o,z,t-1} \ , \forall \ o \in \boldsymbol{O} \ , z \in \boldsymbol{Z} \ , t \in \boldsymbol{T}^{interior}$$

(3-7)

3.2.2 Programming Configuration

A description of the decisions made concerning settings inputs, and variables in the model.

Solver settings

The model is optimized using an educational license for Gurobi, with full solver capability. Settings for Gurobi were mostly set to default to maintain stability in the simulation. Feasibility tolerance (primary constraint tolerance) and optimality tolerance (Dual feasibility tolerance) was set to 1e-5 so as not to differentiate the dual solutions as some of them are useful as results. Pre-solve was set to 2 (aggressive) to achieve a tighter model at the cost of longer solve time as solve time was proven to not be a problem in the project assignment preluding this thesis [71]. The solver method is set to where the solver itself decides what method is best suited for each simulation. This way an optimal solution is most likely. In most cases, the solver used a barrier method together with an LP algorithm. Barrier crossover and convergence tolerances were set arbitrarily high so as to force the solver to a conclusion without terminating. The numerical focus was set to 0 where the solver itself decides to which degree it attempts to manage numerical issues [71].

The solver is configured so as not to utilize the inbuilt time domain reduction feature to preserve as much temporal resolution possible for the results. Further, the model is configured to run in multi-stage investment planning mode with seven stages to represent the time period from now until 2023. This method formulates and solves the simulation as a single deterministic multi-stage investment problem with perfect foresight to determine the least-cost investment path [68]. This method is implemented via a dual dynamic programming algorithm [72].

Input variables

Although the model takes inputs through 10 CSV files only five of them are needed to use the model. The five used flies are documented below. The five files not used are displayed in Table 3-3. None of these inputs are strictly needed for the desired use of the model and are therefore excluded.

Table 3-3 Input files used in the model.

Reserves.csv	Sets operational reserve margin requirements.
Energy_share_requirement.csv	Sets a requirement for least produced power of each resource.
CO2_cap.csv	Sets limit for CO_2 emissions.
Capacity_reserve_margin.csv	Sets requirements for regional capacity reserve margin.
Minimum_capacity_requirement.csv	Sets requirements for least installed capacity for each recourse.

Generator inputs

Sets cost and performance data for storage and generation, and flexibility for each node.

The most important of these specific inputs are documented in Table 3-4. Most of the inputs not presented in Table 3-4 are default values with little to no impact on simulation results. Technical inputs for the generators and batteries are gathered from Arva and Tromskraft and further documented in the Data section of the thesis in Chapter 3.4.3.

The zone is given by the geographical location of the given nodes according to where the largest loads are located. Most of these nodes are situated at the end of distribution radials with load aggregated through the radial into a single point for computational reasons, as simulation time increases exponentially with node amount [68, 73].

Investment costs are the annualized cost of investing, given a certain cost of capital. Operational and maintenance costs are continuously calculated. Hydro energy to power ratio is used in the storage inventory balance constraint within the discharge module presented in Equation (3-8) and Equation (3-9).

$$\Gamma_{y,z,t} = \Gamma_{y,z,t-1} - \frac{1}{\eta_{y,z}^{down}} \theta_{y,z,t} - \varrho_{y,z,t} + \rho_{y,z,t}^{max} \times \Delta_{y,z}^{total} \ \forall \ y \in W, z \in Z, t \in T^{interior}$$

$$(3\text{-}8)$$

$$\Gamma_{y,z,t} = \Gamma_{y,z,t+\tau^{period}+1} - \frac{1}{\eta_{y,z}^{down}} \theta_{y,z,t} - \varrho_{y,z,t} + \rho_{y,z,t}^{max} \times \Delta_{y,z}^{total} \ \forall \ y \in W, z \in Z, t \in T^{start}$$

$$(3\text{-}9)$$

This constraint enforces that the energy level of the reservoir resource y and zone z in time step t, $\Gamma_{y,z,t}$ is defined as the sum of the reservoir level in the previous time step, less the amount of electricity generated, $\Theta_{y,z,t}$ (accounting for the generation efficiency, $\eta_{y,z}^{down}$), minus any spillage $\varrho_{y,z,t}$, plus the hourly inflows into the reservoir (equal to the installed reservoir discharged capacity times the normalized hourly inflow parameter $\rho_{y,z,t}^{max}$). $\Delta_{y,z}^{total}$ denotes the total installed power capacity of the generator. Subscripts y, z, and t denotes resource, zone, and timestep, respectively.

The weighted average cost of capital for each technology is utilized to calculate the capital recovery period, set to be the same as the lifetime of each device. The cost of capital is set by the expected change in interest rates governed by the Norwegian central bank and lifetime is set as industry averages [53, 74].

Table 3-4 Most important attributes in the Generators.csv input file.

Zone	Hydro	New Build
Depicts what zone in the network each implemented technology.	Flags if a technology is hydroelectric, as other variables are dependent on this.	Flags if a technology is a new build or if it was already installed before the simulation period.
Existing_Cap_MW	**Existing_Cap_MWh**	**Existing_Charge_Cap_MW**
The existing capacity of a power plant in megawatts.	The existing capacity of devices flagged as storage, in megawatt hours.	The existing charging capability of devices flagged as storage, in megawatts.
Max_Cap_MW	**Max_Cap_MWh**	**Max_Charge_Cap_MW**
The maximum installable capacity of a power plant in megawatts.	The maximum capacity of devices flagged as storage, in megawatt hours.	The maximum capacity of devices flagged as storage, in megawatts.
Min_Cap_MW	**Min_Cap_MWh**	**Min_Charge_Cap_MW**
The minimum installable capacity of a power plant in megawatts.	The minimum capacity of devices flagged as storage, in megawatt hours.	The minimum capacity of devices flagged as storage, in megawatts.
Inv_Cost_per_MWyr	**Inv_Cost_per_MWhyr**	**Fixed_OM_Cost_per_MWyr**
Annualized capacity investment cost of a technology in 1/megawatts/year.	Annualized investment cost of the energy capacity for a storage technology in 1/megawatt hours/year.	Fixed operations and maintenance cost of a technology in 1/megawatts/year.
Start_Cost_per_MW	**Hydro_Energy_to_Power_Ratio**	**Eff_Up / Eff_Down**
Fixed operations and maintenance cost related to starting a technology, in 1/megawatt/year. Multiplied by the number of generation units.	The rated number of hours of reservoir hydro storage at peak discharge power output.	Efficiency of charging and discharging as a percentage of utilization.
WACC	**Capital_Recovery_Period**	**Lifetime**
Weighted average cost of capital given as a percentage.	Estimated time before investment cost is repaid through earnings.	Estimated lifetime of installed device.

Network inputs

Network inputs are mainly a method of describing the topology of the regional network and the distribution network. This is presented as a matrix map with n columns, one per zone, with column header in the format of z* where * is the number of the zone. L rows, one for each network line (or interregional path), with a 1 in the column corresponding to the 'origin' zone and a -1 in the column corresponding to the 'destination' zone for each line. No more than one column is marked as the origin and one as the destination for each line. Note that positive flows indicate flow from the origin to the destination zone; negative flows indicate flow from the destination to the origin zone. Maximum line flow is set in megawatts with loss set as a percentage of measured flow at any time interval. There are also inputs for line reinforcement, but these are not utilized as none of the scenarios take account of line reinforcement [68]. The network map is presented in Table 3-6.

Transmission loss is added to the power balance of each zone as a term shown in Equation (3-10).

$$\sum_{l \in \boldsymbol{L}} \left(\varphi_{l,z}^{map} \times \Phi_{l,t}\right) - \frac{1}{2} \sum_{l \in \boldsymbol{L}} \left(\varphi_{l,z}^{map} \times \beta_{l,t}(\cdot)\right)$$

(3-10)

Where $\beta_{l,t}(\cdot)$ denotes the loss factor of each line segment. With loss calculated linearly as shown in Equation (3-11) with power magnitude calculated as in Equation (3-12).

$$\beta_{l,t}(\cdot) = \varphi_l^{loss} \times \left|\Phi_{l,t}\right|, \forall \, l \in \boldsymbol{L}, \forall \, t \in \boldsymbol{T}$$

(3-11)

With φ_l^{loss} as a set percentage loss of the magnitude of power flow in each line $\left|\Phi_{l,t}\right|$.

$$\Phi_{l,t} = \Phi_{l,t}^+ - \Phi_{l,t}^- , \forall \, l \in \boldsymbol{L}, \forall \, t \in \boldsymbol{T}$$

$$\left|\Phi_{l,t}\right| = \Phi_{l,t}^+ - \Phi_{l,t}^- , \forall \, l \in \boldsymbol{L}, \forall \, t \in \boldsymbol{T}$$

$$\Phi_{l,t}^+ - \Phi_{l,t}^- \le \varphi_l^{max} , \forall \, l \in \boldsymbol{L}, \forall \, t \in \boldsymbol{T}$$

(3-12)

Here $\Phi_{l,t}^+$ and $\Phi_{l,t}^-$ denotes power flow in the positive and negative direction respectively. Subscript l denotes line segment and t denotes timestep.

Load inputs

Load inputs are presented in Table 3-5.

The value of lost load is used as a means to nudge the model towards always delivering the demanded amount of power. As parts of the industry in Senja demands high-quality power without risk of outages, the value of lost load is majorly increased from its default value. Curtailment factors are presented in the load inputs and calculated in the model as a constraint shown in Equation(3-13).

$$\theta_{y,z,t} \leq \sum_{(x,z),\in vre_{x,y}} \rho_{x,z,t}^{max} \times \Delta_{x,z}^{total}, \forall\, y, z \in \{(y,z)|vre_{y,z} = 1, z \in Z\}, t \in T$$

(3-13)

Where $\rho_{x,z,t}^{max}$ denotes resource quality and $\Delta_{x,z}^{total}$ denotes retired capacity.

The time index spans every hour of the given year within the simulation. The load matrix is constructed with figures further discussed in Chapter 3.4.1.

Table 3-5 Most important attributes in the Load.csv input file.

Voll	Demand_Segment	Cost_of_Demand_Curtailment
Value of lost load in 1/MW	Number of demand curtailment/lost load segments with different cost and capacity of curtailable demand for each segment.	Cost of non-served energy/demand curtailment (for each segment), reported as a fraction of value of lost load.
Max_Demand_Curtailment	**Time_Index**	**Load_Matrix**
Maximum time-dependent demand curtailable in each segment, reported as % of the demand in each zone and each period.	Index defining time steps in the model.	If multiple zones, this parameter will be a matrix with columns equal to number of zones (each column named appropriate zone number appended to parameter) and rows equal to number of time periods of grid operations being modeled.

Fuel inputs

Fuel inputs set the price and availability of fuels. None of the implemented technologies use fuel, leaving this as an empty time series matrix.

Generator variability inputs

Inputs for generator variability are made up of a time index defining time steps in the model, with one step for each hour in the year and a matrix with a column for each implemented technology. Each column is filled with float numbers between 1 and 0, depicting the percentage of maximum power available for each device. For hydropower plants, this number is always 1 as a hydropower plant can run at full power as long as there is water in the reservoir. For VRE sources numbers have been generated with a normal distribution based on yearly average use-hours of wind and solar in Norway through simple Python code seen in Appendix A [53].

Objective function

The objective function used in the model can be seen in Equation (3-14).

$$
\begin{aligned}
min \sum_{y\in G}\sum_{z\in Z} & \left[\left(\pi_{y,z}^{INVEST}\times\overline{\Omega_{y,z}^{size}}\times\Omega_{y,z}\right)+\left(\pi_{y,z}^{FOM}\times\overline{\Omega_{y,z}^{size}}\times\Delta_{y,z}^{total}\right)\right] \\
& +\sum_{y\in O}\sum_{z\in Z}\left[\left(\pi_{y,z}^{INVEST,energy}\times\Omega_{y,z}^{energy}\right)+\left(\pi_{y,z}^{FOM,energy}\times\Delta_{y,z}^{total,energy}\right)\right] \\
& +\sum_{y\in O^{asym}}\sum_{z\in Z}\left[\left(\pi_{y,z}^{INVEST,charge}\times\Omega_{y,z}^{charge}\right)+\left(\pi_{y,z}^{FOM,charge}\times\Delta_{y,z}^{total,charge}\right)\right] \\
& +\sum_{y\in G}\sum_{z\in Z}\sum_{t\in T}\left[\omega_t\times\left(\pi_{y,z}^{VOM}+\pi_{y,z}^{FUEL}\right)\times\Theta_{y,z,t}\right] \\
& +\sum_{y\in O\cup DF}\sum_{z\in Z}\sum_{t\in T}\left[\omega_t\times\pi_{y,z}^{VOM,charge}\times\Pi_{y,z,t}\right] \\
& +\sum_{s\in S}\sum_{z\in Z}\sum_{t\in T}\left[\omega_t\times n_s^{slope}\times\Lambda_{s,z,t}\right]+\sum_{t\in T}\left[\omega_t\times\pi_{rsv}^{unmet}\times r_t^{unmet}\right] \\
& +\sum_{y\in H}\sum_{z\in Z}\sum_{t\in T}\left[\omega_t\times\pi_{y,z}^{START}\times\chi_{s,z,t}\right]+\sum_{l\in L}\left[\pi_l^{TCAP}\times\Delta\varphi_l^{max}\right]
\end{aligned}
$$

(3-14)

With annualized capital cost $\pi_{y,z}^{INVEST}$, fixed operational and maintenance cost $\pi_{y,z}^{FOM}$, net installed capacity $\overline{\Omega_{y,z}^{size}}\times\Delta_{y,z}^{total}$, annualized energy capital cost $\pi_{y,z}^{INVEST,energy}$, fixed operational and maintenance energy cost $\pi_{y,z}^{FOM,energy}$, total storage capacity $\Delta_{y,z}^{total,charge}$, fixed charging cost $\pi_{y,z}^{INVEST,charge}$ and $\pi_{y,z}^{FOM,charge}$, variable charge cost $\pi_{y,z}^{VOM}$, fuel cost $\pi_{y,z}^{FUEL}$, the weight of each time step ω_t, flexible demand $\Pi_{y,z,t}$, marginal value of consumption n_s^{slope}, non-served energy $\Lambda_{s,z,t}$, cost unmet reserve requirements π_{rsv}^{unmet}, amount of non-served energy r_t^{unmet}, startup cost π_t^{START}, number of startup events $\chi_{s,z,t}$, cost of line construction π_l^{TCAP}, and line reinforcement $\Delta\varphi_l^{max}$. As for subscripts, **G** denotes resources, **Z** denotes zones, **O** denotes storage, **T** denotes timesteps, **S** denotes non-met demand, **H** denotes thermal resources, and **L** denotes line segments.

The objective function comprises several summations that represent the fixed and operational costs associated with different decisions in the power system. The first summation includes the fixed costs of generation and discharge across all zones and technologies, while the second and third summations correspond to the fixed costs of installed energy storage and charging power capacity, respectively. The fourth and fifth summations represent the operational costs across all zones, technologies, and time steps, with the former including fuel and variable O&M costs for energy generation or discharge and the latter including variable charging O&M costs for energy withdrawn for charging. The sixth summation represents the total cost of unserved demand, while the seventh summation represents the total cost of not meeting hourly operating reserve requirements. The eighth summation corresponds to the startup costs incurred by technologies subject to unit commitment decisions, and the last term represents the transmission reinforcement or construction costs [68].

Overall, the objective function aims to minimize costs associated with decisions related to capacity investment, capacity dispatch, consumer demand segments, thermal units, and

transmission network capacity. The optimization is performed over the entire problem as a monolithic co-optimization problem, and the objective function can also be understood as a social welfare maximization problem. The bulk of demand is treated as inelastic and always served, while the utility of consumption for price-elastic consumers is represented as a segment-wise approximation.

3.3 Scenario Description

Scenarios for this thesis are based on what aspects of the electrical grid are of interest to the grid owner, local power producer, and the scientific community. Understanding bottlenecks in the network, finding alternatives to network expansion, and understanding the cooperation between local generation and energy storage are all fields of interest [3]. To investigate as many of these aspects as possible, within the limits of a single thesis, three scenarios have been constructed. All three scenarios have been simulated in a high- and low-demand growth scene.

Scenario 1 is a baseline scenario where the model follows today's network configuration as closely as possible without any means of expansion or compensation. Today's configuration includes the newly installed batteries in Senjahopen and Husøy. Having a baseline scenario is useful as a comparison for other scenarios as well as investigating the current network for bottlenecks.

Scenario 2 is meant as a simple expansion example where the model is allowed to expand the network with 1 megawatt wind, 1 megawatt solar PV, and 1 megawatt battery energy storage. These figures are chosen as 1 megawatt is the upper limit of power production allowed without a concession duty assessment from NVE [75].

Scenario 3 is meant as an island operation example where the internal network of Senja is cut off from the external transmission network. In this example, the model is free to expand in any way it seems fit, in order to deliver stable power to all nodes.

Growth scenes are built mainly based on reports from the largest seafood actors, the largest industrial actors, and readings from the grid owner. Seafood energy estimates are presented in Figure 3-4.
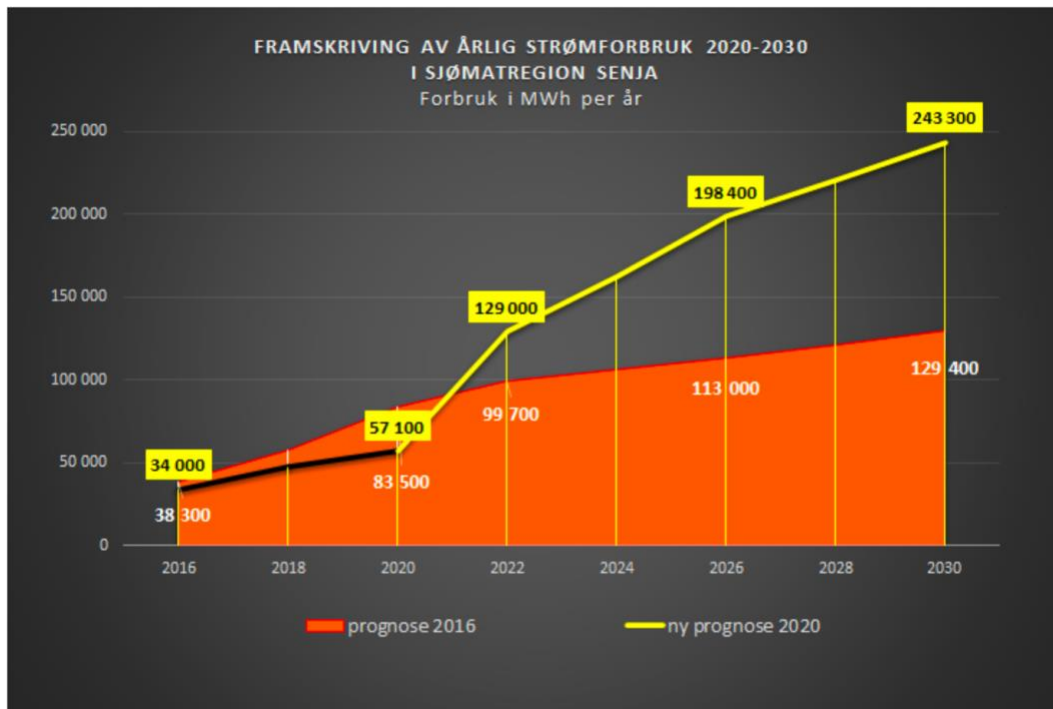
Figure 3-4 Graph showing the growth in electricity use in the seafood industry in Senja.

3.3.1 High growth scene

A scene for each scenario with 15% yearly growth in electricity demand. This scene is based on Statistics Norway's HHMH prognosis for population growth in the area [76]. Sjømatklyngen Senja estimates a rapid growth of fish breeding with hatchery fish as well as electrifying the existing fleet of boats.

3.3.2 Low growth scene

A scene for each scenario with 8% yearly growth in electricity demand. This scene is based on Statistics Norway's MMMM prognosis for population growth in the area [76]. Considering the high congestion in the electricity network the growth in fish breeding is somewhat lessened, and only small changes in the existing fleet of boats are expected. The result of these considerations, growth in electricity demand is dramatically lower than the high growth scene.

3.4 Data Collection and Handling

Load data from every network station, transformer station, and power line on Senja as of 2019 was provided by Arva as Excel files. Ten files were provided, and five of these contained useful information for the thesis. The files not used had data for the generators at Senja, which was gathered from Tromskraft produksjon, readings for the regional network, and in-depth data for the transformer stations. As the transformer loss was deemed neglectable, these data were of no use. The regional network of Senja is deemed as a "rigid" network and modeled as such using standard values of 2.5% loss [37].

Generator data have been individually sourced from public records available through the local power producer and through NVE´s web pages [53, 67]. Data for the electricity consumption growth scenes have been collected from local industrial consumers, the local electricity producer, and the grid owner [3, 4, 65, 66].

3.4.1 Load

Two of the ten files had information concerning load and load profiles. Most notable was the dataset for network stations, presented in an 11 X 553 matrix with a separate row for each distinct network station. The columns of the data set represented a set quality of the given network station. Columns are presented in the list below:

- Object number   ~ a distinct seven-digit number for each object in the network.
- Location   ~ a distinct seven-digit location number and name.
- Area   ~ three-digit area number and name.
- Municipality   ~ area code and name of the municipality of the station.
- Owner   ~ name of station owner.
- Station-type   ~ description of build technique.
- Type   ~ description of station model.
- Radial   ~ name of the radial connected to the station.
- Max active power   ~ reading of the highest recorded active power draw.
- Max reactive power ~ reading of the highest recorded reactive power draw.
- Junction   ~ used to distinguish connected cables and lines.

Load data for each distinct network station could not be provided as time series because of privacy policy reasons. Therefore, a load curve had to be applied to produce useful data for the model. Peak load data is scaled to compensate for the asynchronous nature of peak data and added within each radial. To see how the data was scaled see Appendix A. The file used to make hourly data for the model was a load curve from the power line connecting Senja to the external grid, provided as a time series. This is a messy time series with large fluctuations between readings, shown in Figure 3-5. To make a helpful load curve from this, the data has been smoothened out with a rolling average window function over one week of hourly data and normalized with Equation (3-15) [77].

$$\boldsymbol{d_n} = \frac{x}{\max d_D} \, , \forall d_D \in \boldsymbol{D}$$

(3-15)

Where the smoothened value $\boldsymbol{d_n}$ is comprised of a fraction of each load value x divided by the maximum load $\max d_D$, for all load values d_p in the time series **D**.

The post-processed load curve can be seen in Figure 3-6. When applying this load curve to the calculated peak load of each radial, a specific load curve can be constructed. The load curves of each distinct radial can be seen in Figure 3-7.

As seen in Table 3-7, 10 nodes have been selected to cover most of the electricity consumption in the distribution grid. To separate the network stations into the different nodes, they were sorted by their radial marking and grouped. From there, the active power of each station was added to a single integer for each group. This integer was later used to scale the load curve. Not all network stations are included within these zones, resulting in 2% of the total load not accounted for in the model. This load has been evenly distributed between the nodes.
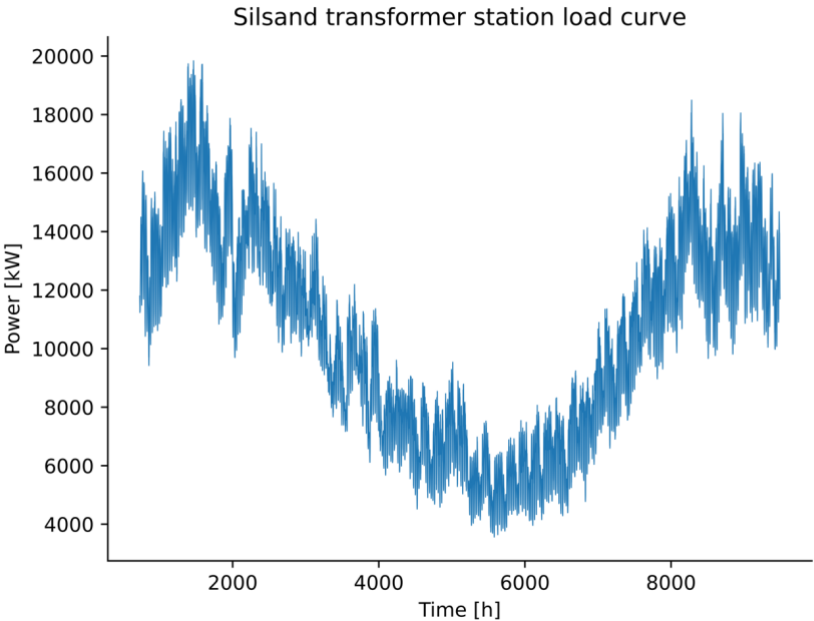
Figure 3-5 Load curve of Senja measured at the transformer station where the sea cable connects the island to the external transmission grid. The x-axis is presented in hours, where hour 1 is the first hour January and hour 8760 is the last in December.
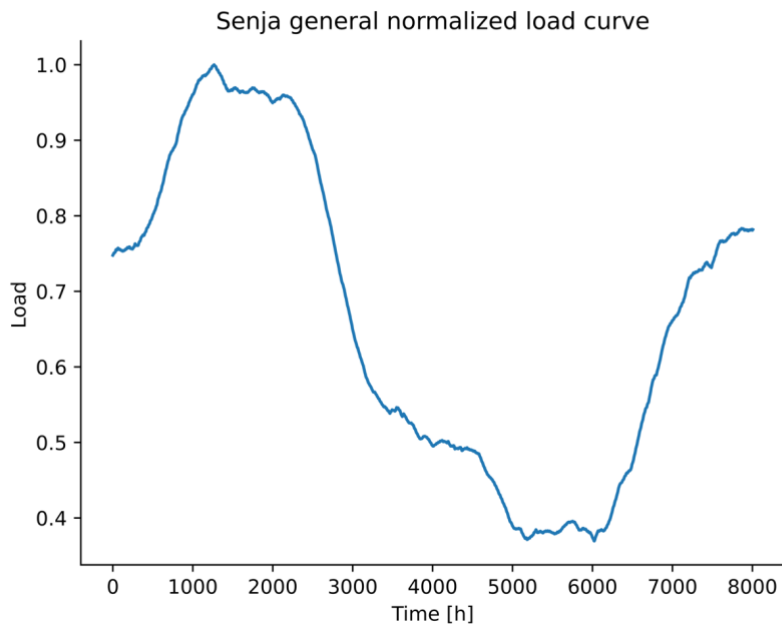
Figure 3-6 Normalized load curve, ready to scale the load of each individual zone. The x-axis is presented in hours, where hour 1 is the first hour January and hour 8760 is the last in December.
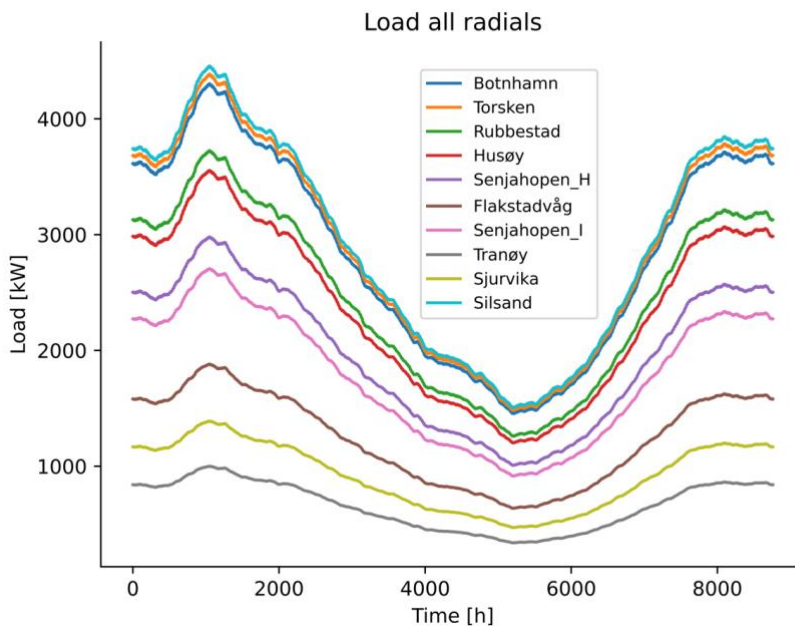
Figure 3-7 Load of each individual zone in year 0, as a function of the normalized load curve scaled my max load in each zone. The x-axis is presented in hours, where hour 1 is the first hour January and hour 8760 is the last in December.

3.4.2 Network

To generate the network data needed for the model, three of the ten provided files were used. The most essential attributes found in these datasheets are presented below:

- Object number ~ a distinct seven-digit number for each object in the network.
- Radial ~ name of the radial of each line.
- Length ~ length of each power line in km.
- Voltage ~ highest voltage measured in each line.
- Current ~ highest measured current in each line.
- Resistance ~ highest measured resistance of each line.
- Reactance ~ highest measured reactance of each line
- Junction 1 ~ used to distinguish connections at one side of the line.
- Junction 2 ~ used to distinguish connections at the other side of the line.

Table 3-6 Regional distribution network layout as portrayed in the model. The lines columns display the number of lines connected to that respective zone. In the matrix, lines are described from zones marked with 1 to zones marked with -1.

| Zone	Lines	Z1	Z2	Z3	Z4	Z5	Z6	Z7	Z8	Z9	Z10	Z11	Z12	Z13	Z14	Z15
Z1	1	-1	0	0	0	0	0	0	0	0	0	0	1	0	0	0
Z2	1	0	-1	0	0	0	0	0	0	0	0	0	0	1	0	0
Z3	1	0	0	-1	0	0	0	0	0	0	0	0	0	0	0	1
Z4	1	0	0	0	-1	0	0	0	0	0	0	0	0	0	0	1
Z5	1	0	0	0	0	-1	0	0	0	0	0	0	0	1	0	0
Z6	1	0	0	0	0	0	-1	0	0	0	0	0	0	0	1	0
Z7	1	0	0	0	0	0	0	-1	0	0	0	0	0	1	0	0
Z8	1	0	0	0	0	0	0	0	-1	0	0	0	0	0	0	1
Z9	1	0	0	0	0	0	0	0	0	-1	0	0	0	0	1	0
Z10	1	0	0	0	0	0	0	0	0	0	-1	0	1	0	0	0
Z11	1	0	0	0	0	0	0	0	0	0	0	1	-1	0	0	0
Z12	4	0	0	0	0	0	0	0	0	0	0	0	1	0	0	-1
Z13	4	0	0	0	0	0	0	0	0	0	0	0	0	-1	0	1
Z14	3	0	0	0	0	0	0	0	0	0	0	0	0	0	-1	1
Z15	6	0	0	0	0	1	0	-1	0	0	0	0	0	0	0	0

Constructing the network topography was done using the network station datasheet and the radial attribute. Every line segment and network station were ordered by radial and sorted by junction number. This way, every element of the network was accounted for, and a comprehensive map of the network was constructed. This construction was then translated to the format used by the model and imported to the network CSV-file. Table 3-6 displays the topography matrix as it is used in the model.

To calculate the maximum transfer capacity of each distribution radial, a reading of the current flow in each line was used. These readings were provided as spot readings of the highest current in each line during the year. As the premise of this thesis is based on an outdated and congested distribution network, this current is used as the highest theoretical current in the network. Maximum power distribution is then calculated with Equation (3-16).

$$P = \sqrt{3} \cdot I_l \cdot V_l$$

(3-16)

With power **P** as a function of line current I_l and line voltage V_l.

Calculating the loss of each radial was done using current flow, resistance and reactance as seen in Equation (3-17). As the current measurements are asynchronous, only the single largest current flow was used for each line with its corresponding resistance and reactance for the measured hour. This tends as a rough simplification for modelling loss in the network but is deemed reasonable within the premise of the thesis.

$$P_l = 3 \cdot I_l \cdot X_l^2 \cdot R$$

(3-17)

Here P_l is the power lost in each line segment.

Loss and other simplifications have been compared to actual loss within the network computed using hourly demand data and generation for the entire island and prove that the simplifications used in the model give results within a margin of error acceptable for a simulation of this extent [35, 49, 59].

Selected properties of the network are displayed in Table 3-7.

Table 3-7 Overview of regional distribution network with power flow figures and calculated line loss.

Radial	Zone	Line_Max_Flow [MW]	Path_Name	Line_Loss
SILS22GI1	Z1	7516	BOTNHAMN	1.79%
STRA22O1	Z2	3194	TORSKEN	0.76%
SVAN22SI1	Z3	6987	RUBBESTAD	1.66%
SVAN22LY1	Z4	5268	HUSØY	1.25%
STRA22SV1	Z5	8406	SENJAHOPEN_I	2%

STON22OS1	Z6	2860	FLAKSTADVÅG	0.68%
STRA22SK1	Z7	5792	SENJAHOPEN_H	1.38%
SVAN22SS1	Z8	1514	TRANØY	0.36%
STON22ST1	Z9	1897	SJURVIKA	0.45%
SILS22SV1	Z10	6537	SILSAND	1.55%
YTTRE_NV	Z11	29000	YTTRE_NETTVERK	2.5%
SILS	Z12	29000	SILSAND_TRAF	2.5%
STRA	Z13	29000	STRAUMSNES_TRAF	2.5%
STON	Z14	29000	STONGLANDSEIDET_TRAF	2.5%
SVAN	Z15	29000	SVANELVMOEN_TRAF	2.5%

3.4.3 Generators and Batteries

Generator data is mainly comprised of public data found through the webpages the owner of the local power plants and webpages describing the cost of energy production in Norway courtesy on the Norwegian water resources and energy directorate [53, 67]. Complementary financial data is collected through reports from the Norwegian central bank [74]. As national economic change is beyond the scope of this thesis, a standard interest rate of 4% has been set for the entirety of the simulation. For simulation purposes a large generator is modeled in the YTTRE_NV zone, set up to be able to produce enough power for the entire island delivered through the regional network. Costs for the external generator are set up to mimic the external power grid. The most significant features in the Generators data sheet are presented in Table 3-8.

Table 3-8 Most significant attributes in the Generators dataset.

Name	Zone	Existing Cap	Inv_cost [MWyr]	OM_cost [MWyr]	Energy ratio	Efficiency	Lifetime
Lysbotn	1	5.36	17461	400	1579	1	50
Bergsbotn	5	8.00	17461	400	2482	1	50
Osteren	2	2.52	17461	400	1015	1	50
YTTRE	11	50000	15306	400	50000	1	50
HU_Batt	4	2.00	10700	107	0	0.86	15

SH_Batt	5	0.80	10700	107	0	0.86	15
Battery	any	0	10700	107	0	0.86	15
Solar	any	0	6000	0	0	0.13	30
Wind	any	0	10071	1000	0	0.46	25

4 Results & Discussion

4.1 Big Picture

This thesis is based on investigating three scenarios built on finding a solution to the electrical energy situation at Senja today. With an eldering electrical network and lacking capacity, industrial and household users are experiencing problems with their electrical energy delivery. As a solution to this problem, modern optimization software has been used to simulate today's electrical network in the future. Two scenarios investigate the impact of installing local electrical green energy production to compensate for the lack of regional distribution capacity.

Figure 4-1 shows a map of all zones in the model area, with numbers. For zone names, see Table 3-1.

Figure 4-1 A map of the model area where zones are marked with numbers. Zones 1-10 are load nodes, while zones 11-15 are junction nodes.

The model has found optimal solutions to this problem with no downtime in the electrical energy distribution. Expanding distributed power production for the low- and high-growth scenes are shown in Figure 4-2 and Figure 4-3 respectively. This local production has positively affected network capacity and is cheaper than today's configuration by a substantial margin. Network capacity has been modeled as static, but no transmission problems have occurred. Relying on local production to a higher degree has decreased the need for external power production and reduced Senja's reliance on its connection to the external transmission grid.

The model proves a possibility for power balance with today's network without extensive short-term energy storage. With the vast expansion of variable energy sources, the need for storage increases, but the strain on the regional electrical network decrease. Even still, the model proves that a network built almost entirely on variable sources can provide the demanded electrical energy through optimal energy flow and storage utilization. This massive expansion of local power production capacity comes with a considerable initial cost but is quickly compensated for by decreased losses and production costs. Conversely, this massive expansion in local production can be non-optimal as curtailment is very high in most zones.
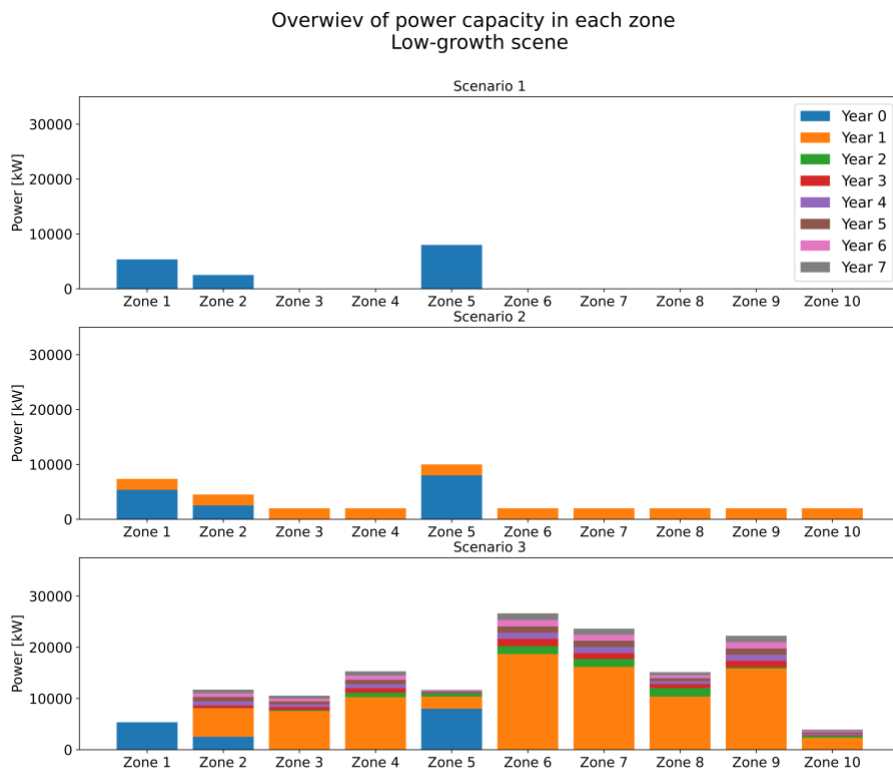

Figure 4-2 Overview of power capacity during all years of all three scenarios in the low-growth scene. Bars represent the installed power capacity of each zone, with colors representing what year that capacity was built.
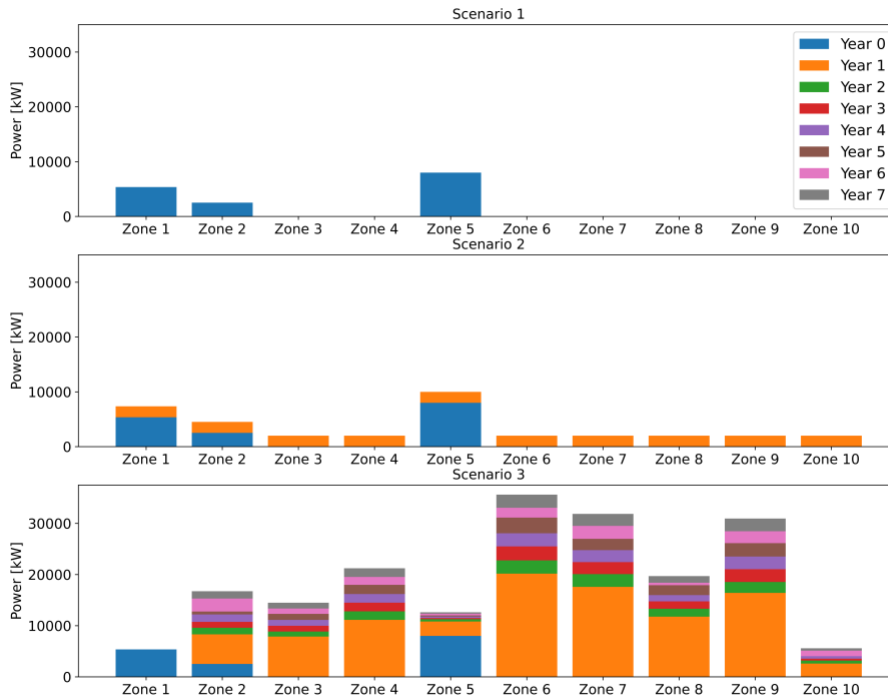
Figure 4-3 Overview of power capacity during all years of all three scenarios in the high-growth scene.

4.2 Power Capacities

This section analyzes how the model chooses to expand upon the current electrical power facilities in Senja. Scenario 1 does not have any power capacity expansion and will stand as a baseline compared to the two other scenarios.

Scenario 1

In scenario 1, installed power capacity is the same as today in both the high- and low-growth scene. There is no added production or storage and no additional power line capacity. Ergo, the electricity system is static throughout the entire modeling period. The total installed capacity is 18.68MW for both the low- and high-growth scenes, in addition to the import capacity through the external grid. The distribution of power capacity can be seen in Figure 4-2. This distribution is the same for the high- and low-growth scenes.

Scenario 2

In scenario 2, the installed power capacity is higher than in scenario 1 because every zone now has added 1MW solar PV, 1MW wind, and 1MW battery. The total installed capacity in this scenario is 48.68MW for both the high- and low-growth scenes, in addition to the import capacity through the external grid. This is 2.6 times higher than scenario 1. The installed

power capacity of each zone in every year of the modeling period is displayed in Figure 4-2 and Figure 4-3 for the low- and high-growth scenes, respectively. The distribution is equal in both scenes.

Scenario 3

In scenario 3, power capacity expansion is very high due to the absence of imported power. Capacity expansion for each zone in the high- and low-growth scenes are displayed in Figure 4-3 and Figure 4-2 respectively. It is apparent from the figures that power capacity is much higher in Scenario 3 than in Scenario 1 or 2. In the high-growth scene, the power capacity is 11.2 times higher than scenario 1 and 4.3 times higher than scenario 2. In the low-growth scene, power capacity is 8.4 times higher than scenario 1 and 3.2 times higher than scenario 2. Power capacity in year one of the high-growth scene is 6.6% higher than in the low-growth scene, while in year seven the difference is 33.1%. This difference in expansion rate is clarified in Figure 4-4 where one can see that expansion is increasing every year in the high-growth scene, whereas in the low-growth scene, the expansion rate decreases. As the lines in Figure 4-4 represent year over year change in power expansion rate, it is evident that in the high-growth scene power capacity is increasing more for each year while the low-growth scene sees less power capacity expansion each year.
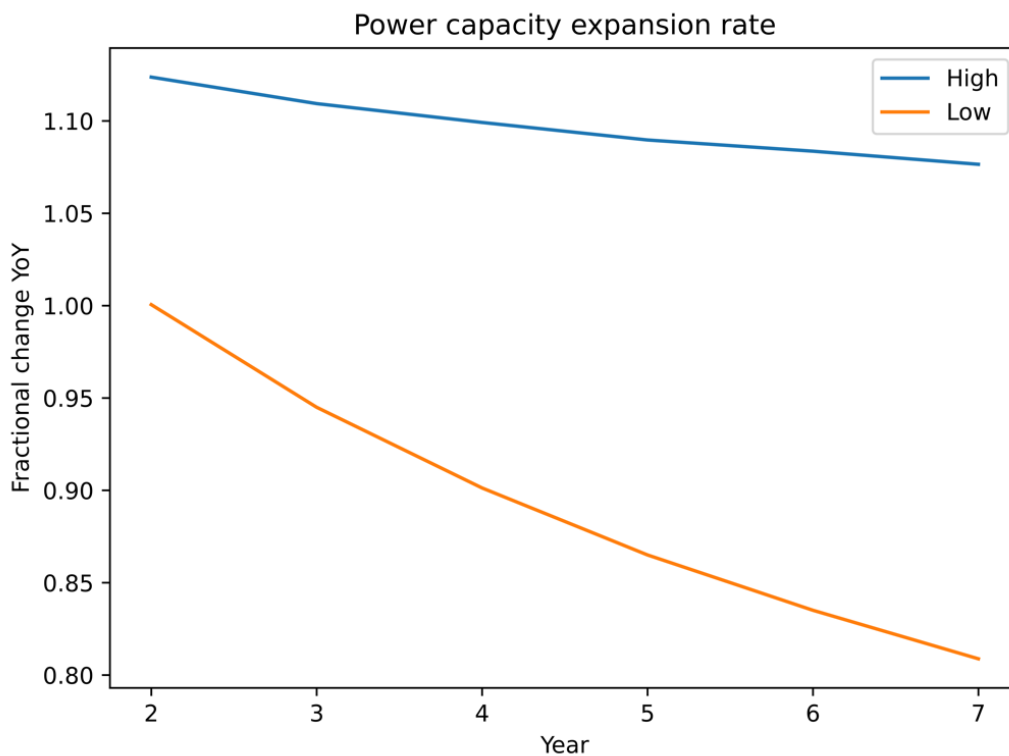

Figure 4-4 Rate of expansion for the entire model area in scenario 3. Change is measured year over year, beginning with the difference between years one and two. The figure displays both scenes, namely the high-growth scene in blue and the low-growth scene in orange.

4.3 Energy Flow

This section investigates how the energy flows in the electrical network and how much energy is lost in transmission and distribution. The section also covers how much each zone generates and to what degree each zone can cover its electrical energy demand.
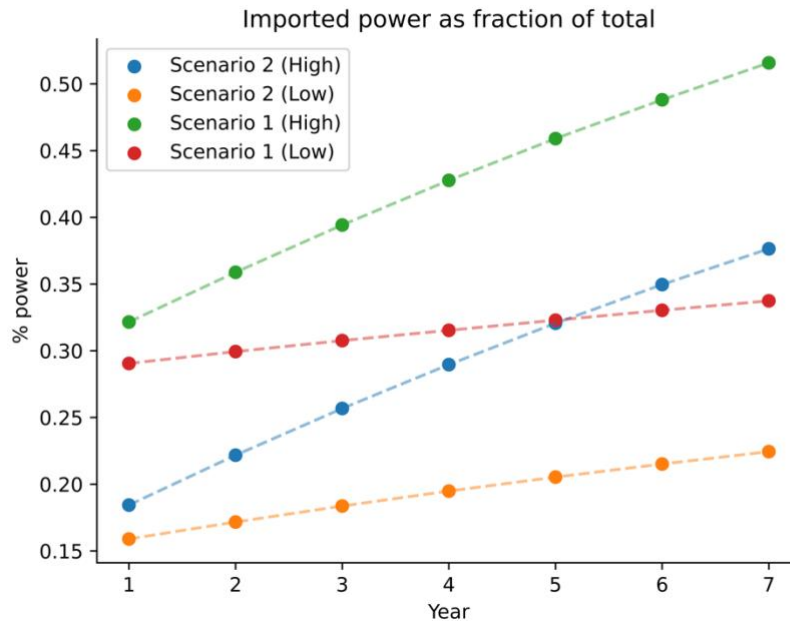
Figure 4-5 Display of imported power for the entire modeled area for all modeled years for scenarios 1 and 2 in both the high and low growth scene. Dots are actual readings, and dashed lines are extrapolations to illustrate tendencies.

Scenario 1

In scenario 1, all original power plants produce much more energy than the yearly average. Yearly production values for Lysbotn, Bergsbotn, and Osteren are on average 68%, 224%, and 59% higher than reported values, respectively, in both growth scenes. Production has very low volatility and minor deviations between summer and winter, especially in the high-growth scene as seen in Figure 4-6. All dips in production are during summer when demand is lower than average. There is a substantial difference in volatility between the low-growth and high-growth scene, as in the low-growth scene there are more hours in the year where the generators can be turned off to reduce operational costs.

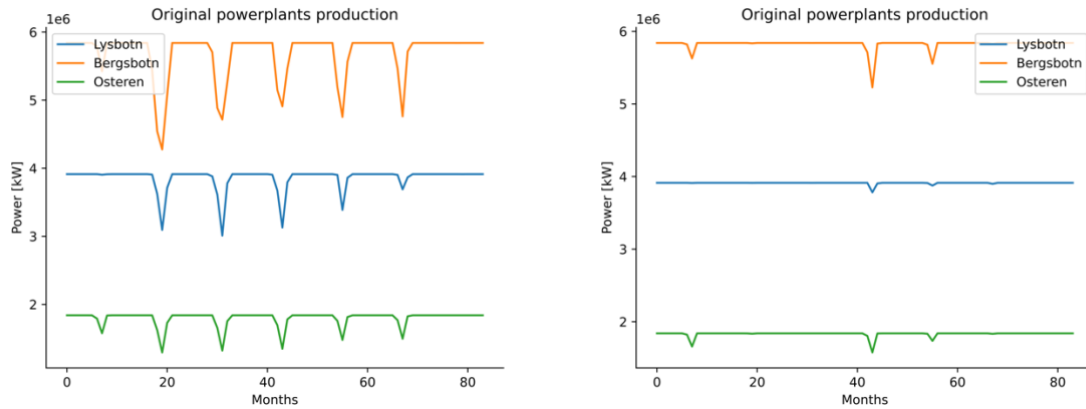*Figure 4-6 Power production of the power plants installed before the model starts for scenario 1 with the high- and low-growth scenes to the right and left, respectively. Osteren is located in Zone 2, Bergsbotn in Zone 5, and Lysbotn in Zone 1. The lines represent power production aggregated on a monthly basis.*

In scenario 1, imported power represents 32.16% of total production in year one of the high-growth scene and 52.58% in year seven. In the low-growth scene imported power represents 30.17% in year one and 41.13% in year seven. Imported power for all years in scenario 1, high and low scenes can be seen in Figure 4-5.

A typical week in the summer and in the winter is displayed in Figure 4-7, depicting how the three generators work in conjunction with the external network to meet the electrical power demand. Local production was enough to cover the demand during this specific week of the summer, and no external power was supplied. In February much of the supplied power is imported from the external transmission network. As seen in Figure 4-7, demand is always met, including transmission loss. These snapshots are collected from close to the 40 and 35 marks on the x-axis of Figure 4-6, ergo July and February in the 4th year of the simulation. As seen in the summer snapshot there is very little battery usage. Only in selected hours the battery kicks in to keep supply up. This is a trend further substantiated in scenarios 2 and 3.
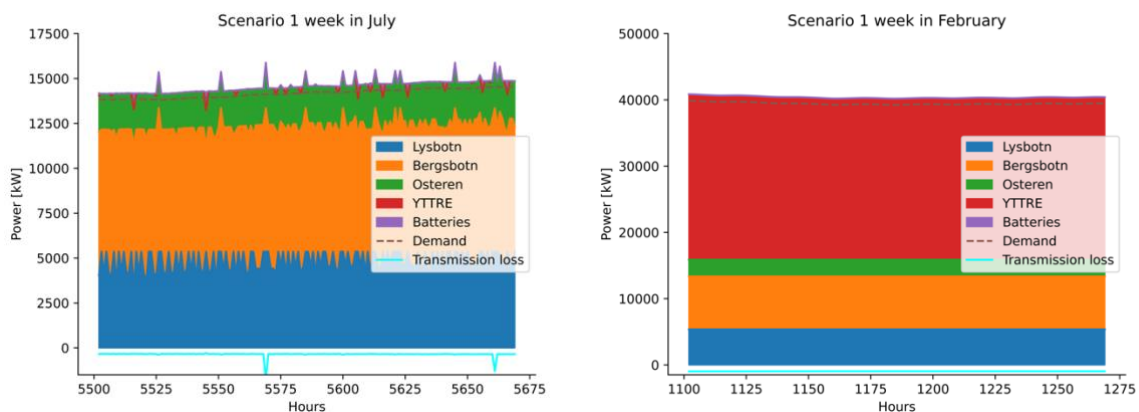
Figure 4-7 Snapshot of power production during a selected week in July and February for scenario 1. This is a cumulative stacked plot of production compared to demand. Note the difference in scale on the y-axis. The dashed line for demand near the top can be hard to spot. The cyan line in the bottom depicts negative values for transmission loss. This loss Is made up for by production, as seen by the stack being taller than the dashed line for demand. YTTRE denotes the external grid.

Scenario 2

In scenario 2, all original power plants produce more energy than the yearly average but less than in scenario 1. Yearly production values for Lysbotn, Bergsbotn, and Osteren are on average 64%, 202%, and 49% higher than reported values in both growth scenes. This amounts to a 5% lower overall production than in scenario 1. Even though production is lower, volatility has increased significantly compared to scenario 1, as seen in Figure 4-8.
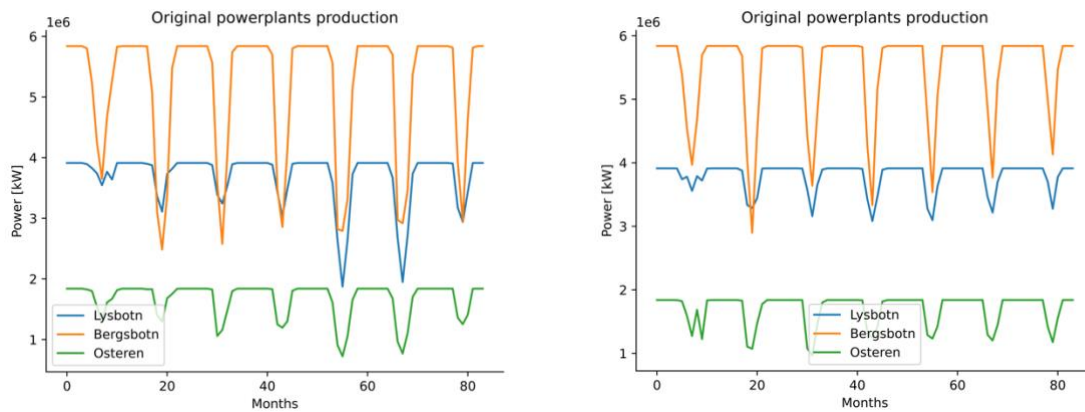
Figure 4-8 Power production of the power plants installed before the model starts scenario 2, with the high- and low-growth scenes to the right and left, respectively.

In scenario 2 imported power represents 18.44% of total production in year one of the high-growth scene and 37.64% in year seven. In the low-growth scene imported power represents 16.50% in year one and 27.35% in year seven. Substantially lower than in scenario 1, and much of this is credited to the additional installed power capacity. Imported power for all years in scenario 2, high and low scenes can be seen in Figure 4-5.

Evidently, the need for power import substantially decreases when local production increases.

Figure 4-9 showcases the increased volatility in scenario 2, where the hydroelectric power plants must fill in when demand is not met through the cheaper VRE sources. In Figure 4-9, it is apparent that transmission loss is much more significant in summer than in scenario 1, as the zones distribute power to each other according to where power production is high. Most of this loss is situated in the distribution network. Comparing this to scenario 3 and Figure 4-11, where the use of VRE is high but demand is met within each zone by local power. In the big picture, these variations are washed out, and as seen in Figure 4-12 transmission loss is not much more significant overall for each year in scenario 2, compared to scenarios 1 and 3. The pink color in Figure 4-9 shows that battery power has increased from scenario 1 and now delivers a higher amount of small power bursts to keep supply above demand. This increase in battery utilization is not apparent in the February snapshot where the pink line is near zero across all hours. Figure 4-9 also highlights the variability in hydroelectric generation where the green color representing Osteren powerplant in Zone 2 is rapidly turning on and off, which can be a deterring factor for the owner of the powerplant as this switching can be damaging for the machine.

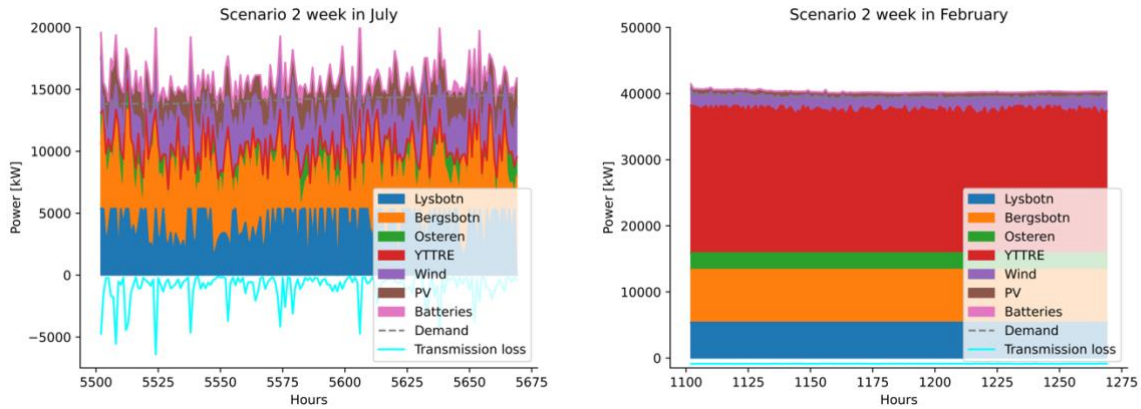*Figure 4-9 Snapshot of power production during a selected week in July and February for scenario 2. Note the difference in scale on the y-axis.*

Scenario 3

In scenario 3 production of the original power plants is much more volatile than in scenarios 1 and 2, but at all times lower in magnitude than in scenario 1. This volatility is apparent in both Figure 4-10 and Figure 4-11 compared to Figure 4-6 and Figure 4-9.
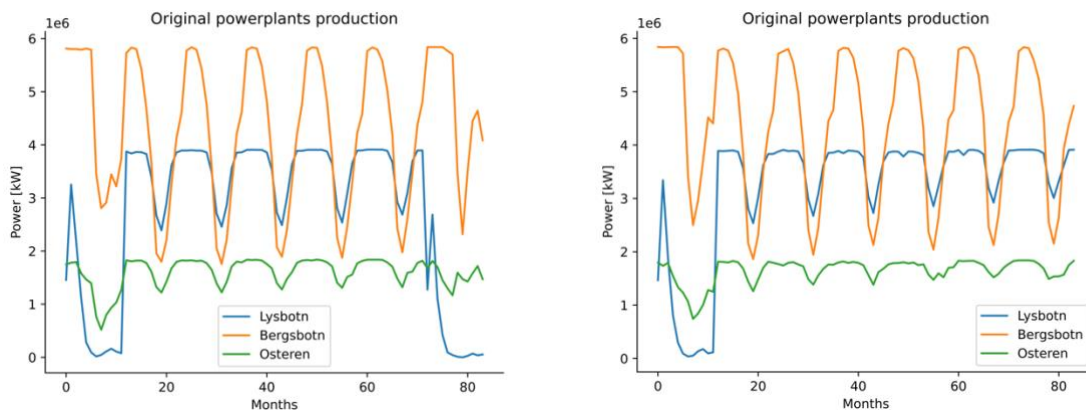
Figure 4-10 Power production of the power plants installed before the model starts scenario 3, with the high- and low-growth scenes to the right and left, respectively.

In scenario 3 the local grid has no external connection to balance the power. It must therefore utilize the local production and storage to a greater degree than in the other two scenarios. Figure 4-11 displays how the model uses all power sources to keep demand and supply in balance. Evidently, demand is always met. In summer the production is controlled by the hydroelectric generators, whereas in the winter VRE sources are responsible for the bulk of production. Figure 4-10 shows how the model must prioritize the value of water differently from scenario 1, as there is no longer an external transmission network available to balance supply and demand. The purple color representing battery use in Figure 4-11 is less prominent than expected as most of the energy is delivered from variable sources. Evidently the model is prioritizing to curtail VRE resources over utilizing batteries for power balance. The cyan line marking transmission loss is notably less volatile compared to scenario 2 indicating that transmission loss in the distribution network is decreased.
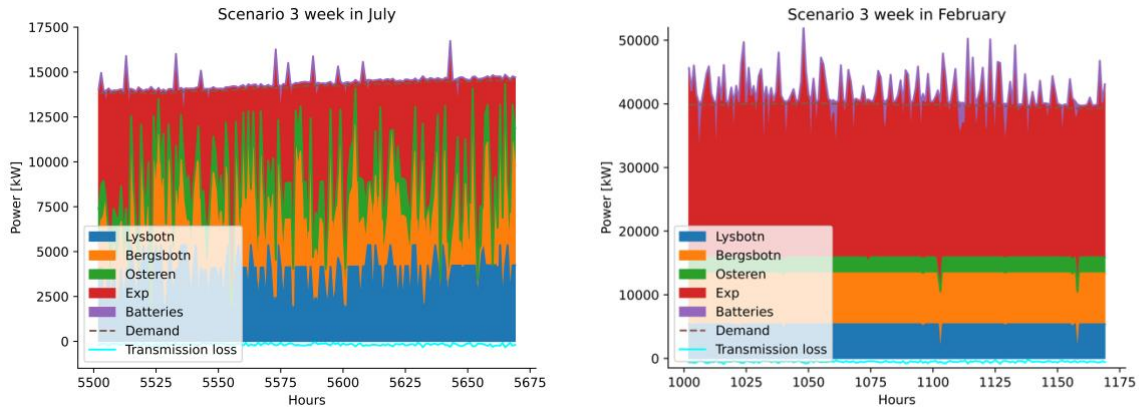
Figure 4-11 Snapshot of power production during a selected week in July and February for scenario 3. Note the difference in scale on the y-axis. Exp denotes the aggregated production of both wind and PV sources.
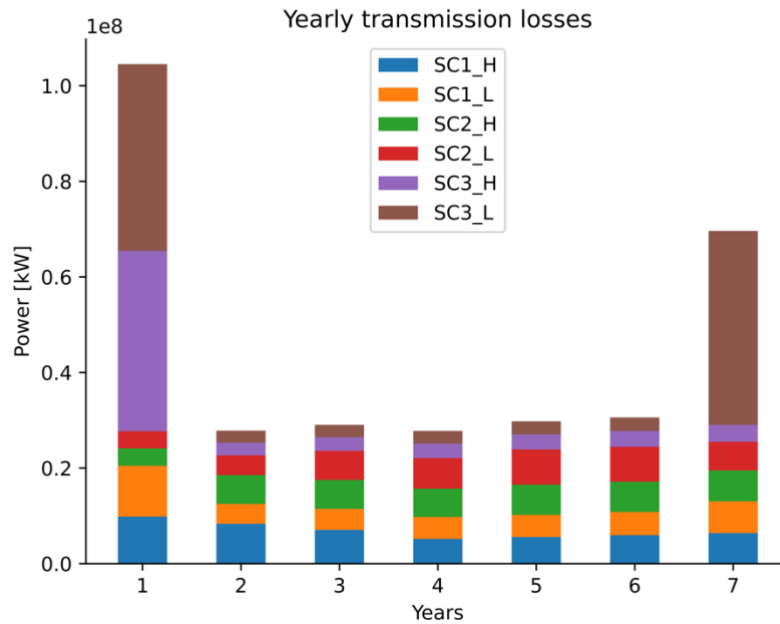
Figure 4-12 Transmission losses for all scenarios in both scenes. For simplicity scenario is shortened to SC and high- and low-growth scenes are denoted as H and L, respectively. Note that all scenarios are separate, and the stacked nature of the figure is only for comparison. Scenario 3 high- and low-growth scene year one is not to size due to a calculation error in the model, and the same is true for scenario 3 low-growth scene.

4.4 Energy Storage

This section investigates how the system utilizes energy storage and to what degree energy demand is met through stored energy.

Scenario 1

The baseline scenario includes 1.8MW of lithium-ion battery storage. Located 1MW in Husøy (Zone 4) and 0.8MW in Senjahopen (Zone 5). Total energy capacity is 1.8MWh, distributed as 1MWh and 0.8MWh in Husøy and Senjahopen, respectively. Ergo the batteries can provide max power for one hour. This proves to have little to no effect on power balance, as the total delivered power from both batteries represents 0.2% of total power on average across all years in both scenes. Utilization of the batteries in today's system is portrayed in Figure 4-13, where one can see that the batteries are not used to a substantial degree on a monthly basis. Especially when compared to Figure 4-14 and Figure 4-15.

Figure 4-13 Battery power delivery for scenario 1, with the high- and low-growth scenes to the left and right, respectively. Note the stacked nature of the display showcasing the magnitude of power delivered by the batteries. HU denotes the battery on Husøy in Zone 4 and SH denotes the battery in Senjahopen in Zone 5.

Scenario 2

Scenario 2 introduces the possibility of increasing battery storage with 10MW and 10MWh evenly distributed across all zones. The model includes the entirety of this capacity from year 1 in both the high- and low-growth scenes, even though the utilization factor still is low with an average of 0.5% power delivered from batteries across all years in both scenes. Figure 4-14 shows how the batteries installed in today´s system are utilized throughout the years of the simulation. It is apparent that the batteries are most useful during selected periods of the year when demand is high and VRE sources do not cover the demand sufficiently. Also apparent is the effect of increased battery capacity in all zones as the batteries in Husøya and Senjahopen are utilized to a lesser degree than in scenario 1. The power delivery from the original batteries is more evenly spread over the course of the simulation, as there are more batteries available in the radials to balance the variability of wind and PV. The system in scenario 2 is less dependent on two distinct zones for balancing measures, compared to scenario 1.
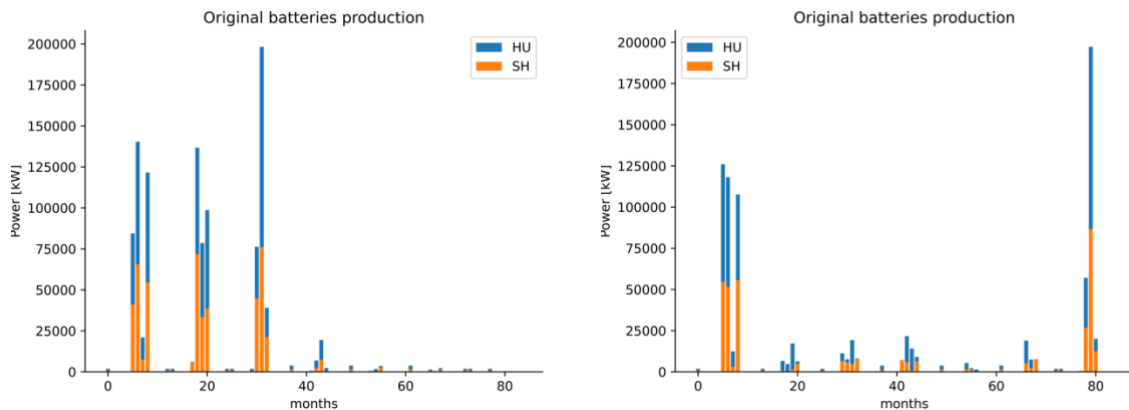
Figure 4-14 Battery power delivery for scenario 2, with the high- and low-growth scenes to the left and right, respectively. Note the difference in scale on the y-axis compared to Figure 4-13 and Figure 4-15.

Scenario 3

Battery utilization in scenario 3 is higher than in both scenario 1 and scenario 2 but still low compared to expectations. Battery utilization for all seven years in both scenes can be seen in Figure 4-15 and Figure 4-16, where utilization is presented as a fraction of overall production in the latter. In Figure 4-15 the same tendencies from scenario 2 become apparent where utilization is high in selected periods of the year, but general use is higher in all months.

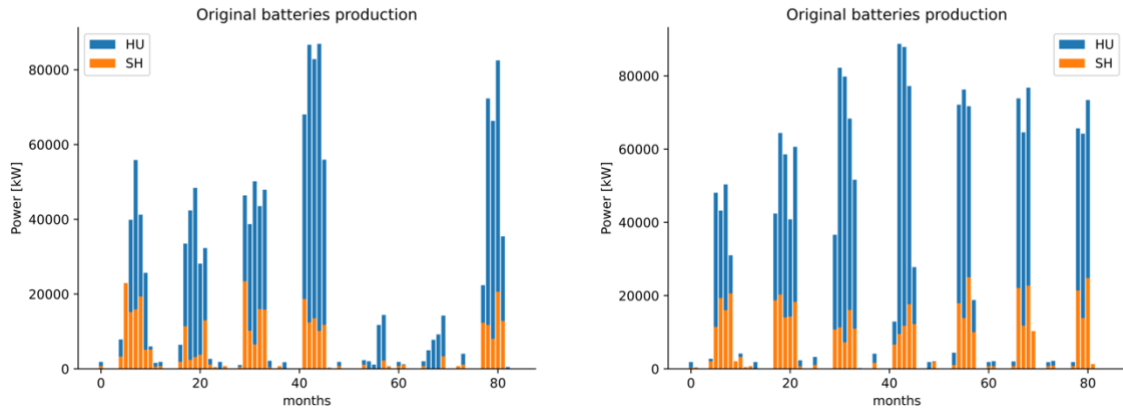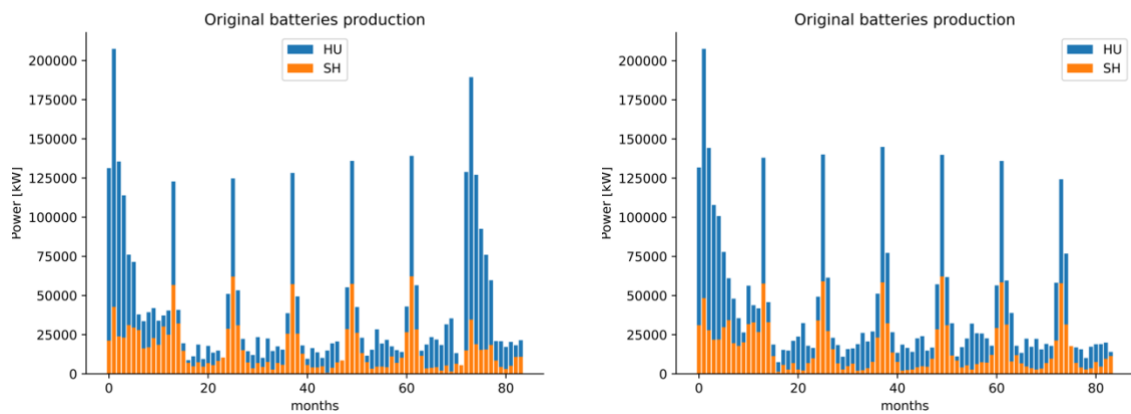*Figure 4-15 Battery power delivery for scenario 3, with the high- and low-growth scenes to the left and right, respectively*
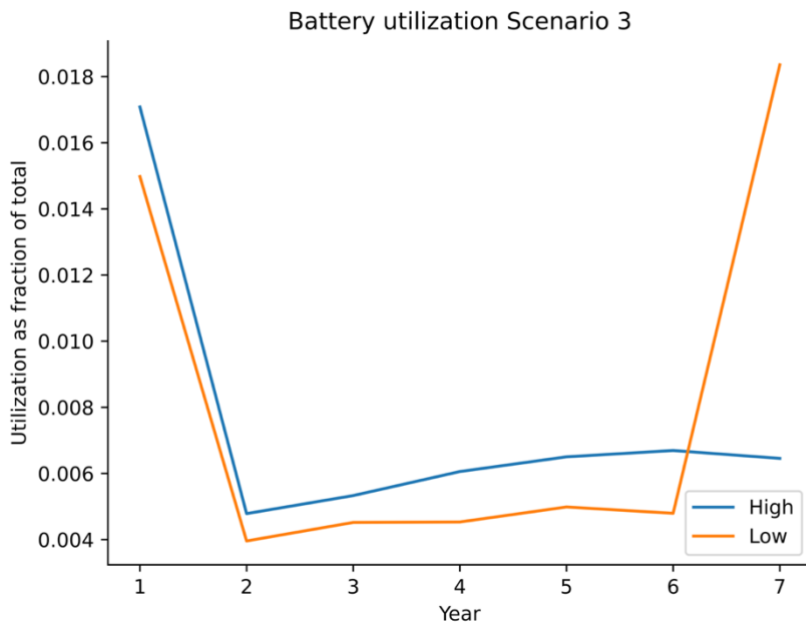
Figure 4-16 Yearly battery utilization of the entire system in both the high- and low-growth scene in scenario 3. Lines represent power delivered by batteries compared to the total power production for each year of the simulation.

4.5 VRE Curtailment

As some sources in the model are depicted as random power sources, the degree of utilization varies as the demand is always known in the model. When demand is lower than what is produced by the variable sources excess energy must be curtailed to not introduce more power than needed to the system. Such overproduction could lead to faults in the network if delivered and is therefore dumped. Curtailment is not penalized in the model in another sense than that building more production than necessary is expensive. When assessing curtailment, production is also considered and the difference between these is measured to give a sense of how well each VRE source is utilized.

Scenario 2

In scenario 2 there are two VRE sources. The utilization of these is displayed in Figure 4-17 and Figure 4-18 for PV and wind power, respectively. As seen in Figure 4-17 PV is underutilized to a high degree in the first years of the simulation period but sees a sharp upswing in year 3. After that, almost all the power produced is sent to the consumer. Wind power is also underutilized in the early years and sees an upswing in use after year 2 for most zones as seen in Figure 4-18. Here it also becomes apparent that zones with low demand utilize wind power to a lesser degree than high-demand zones. This is an effect of the model installing the same capacity in all zones in year 1.
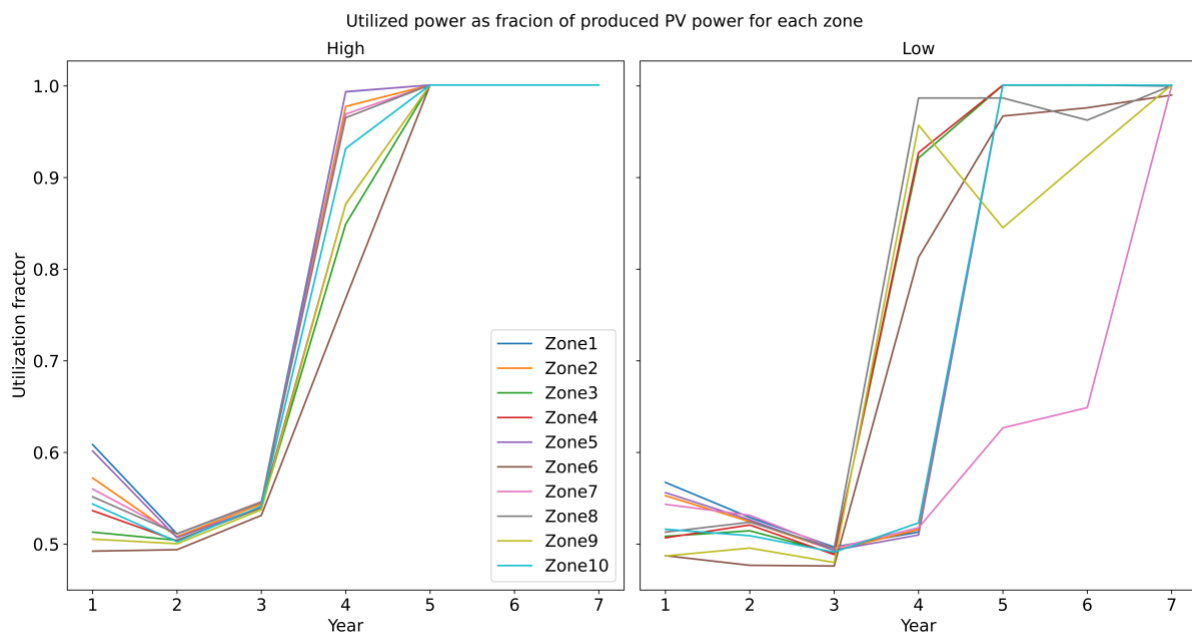
Figure 4-17 Solar power utilization factor as a fraction of production. Utilization factor is comprised of how much power is produced by the PV generators in the system compared to the energy available. The graphs can also be read as the inverse of how much power is curtailed from the PV generators.
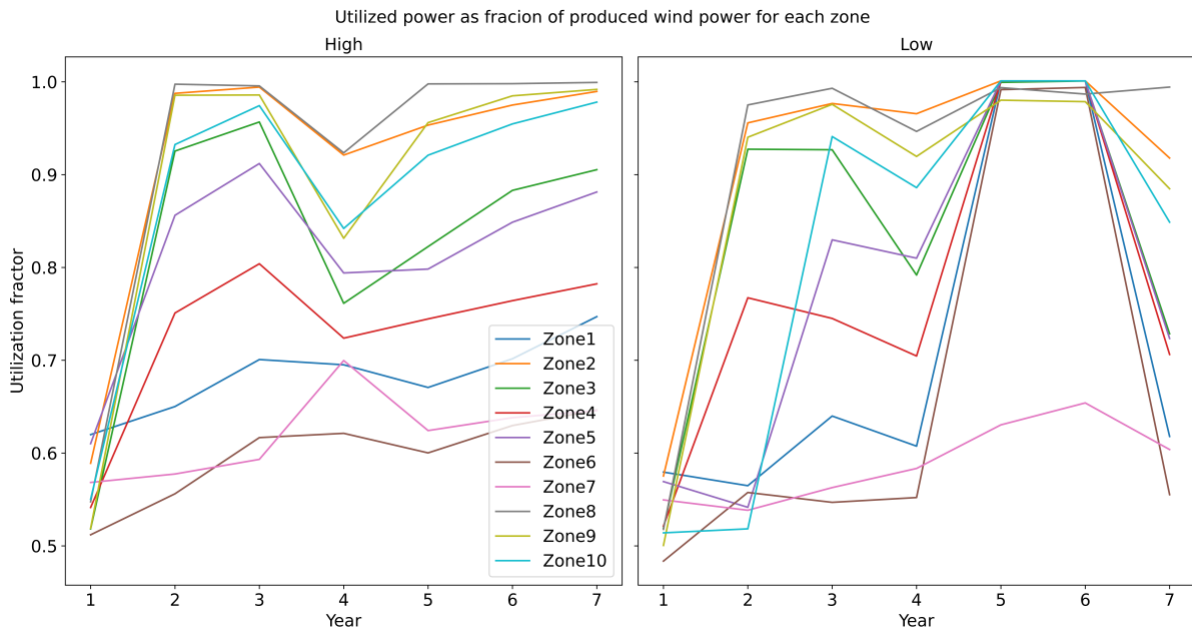
Figure 4-18 Wind power utilization factor as a fraction of production.

Scenario 3

In scenario 3 where VRE sources have a higher penetration one can in Figure 4-19, see a significant difference in utilization between the high- and low-growth scene, where utilization is much lower for the low-growth scene. The high-growth scene VRE source utilization is at a satisfactory level, further proving the possibility of VRE and battery cogeneration. This is further substantiated when analyzing Figure 4-19, Figure 4-15, and Figure 4-16 together.
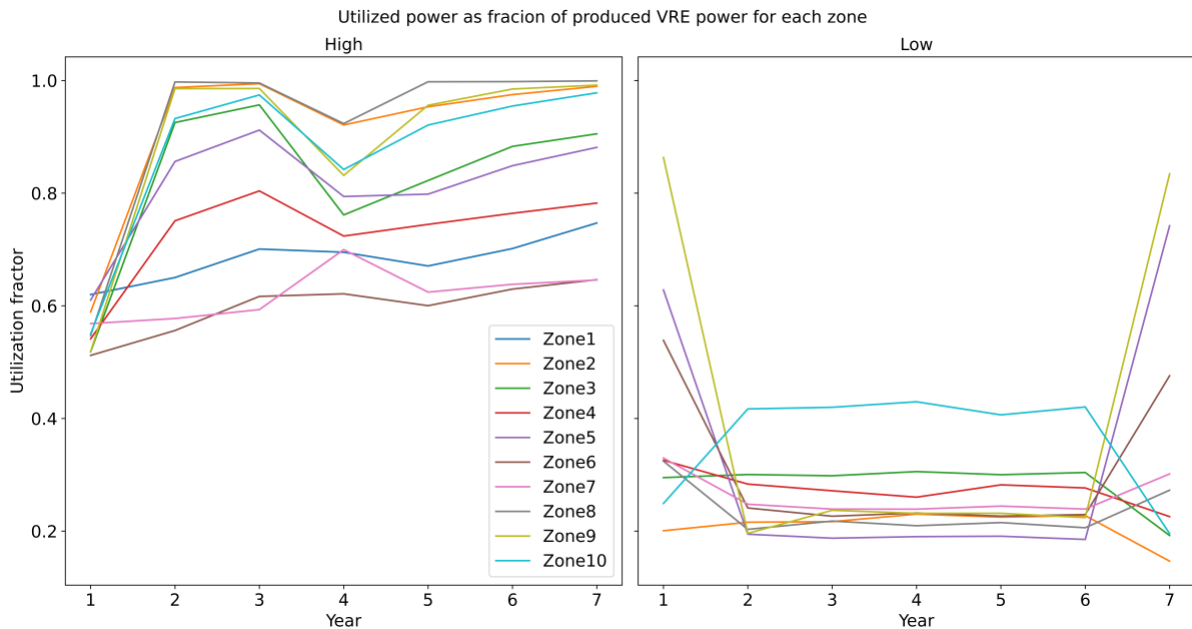
Figure 4-19 VRE source power utilization as a fraction of production.

4.6 System Cost

In this section, the cost in scenarios 2 and 3 are compared to the baseline scenario to analyze the economic value of implementing these system upgrades. As the model has shown a tendency to skew financial calculations and to exercise discretion towards Arva and Tromskraft's financial privacy, only comparisons between scenarios will be presented and not the actual financial status of each scenario.

Scenario 2

System cost is slightly higher than the baseline scenario, as seen in Figure 4-20. A significant change in cost is seen between years 1 and 2 as there is no cost of installation in year 2 and the system then can produce cheap VRE instead of importing electric energy from the external transmission network. Another significance to notice is the difference between the low-growth baseline scenario and the high-growth baseline scenario. When compared to the high-growth baseline scenario the system cost is almost static, with a slight increase in the high-growth scene. Where when comparing to the low-growth baseline there is an apparent increase in system cost in both scenes. Then the high-growth scene in scenario 2 even becomes more expensive than the baseline. This increase in cost could be due to the cost of lost energy in the distribution network, as the model must transfer the locally produced power to other zones with greater demand.
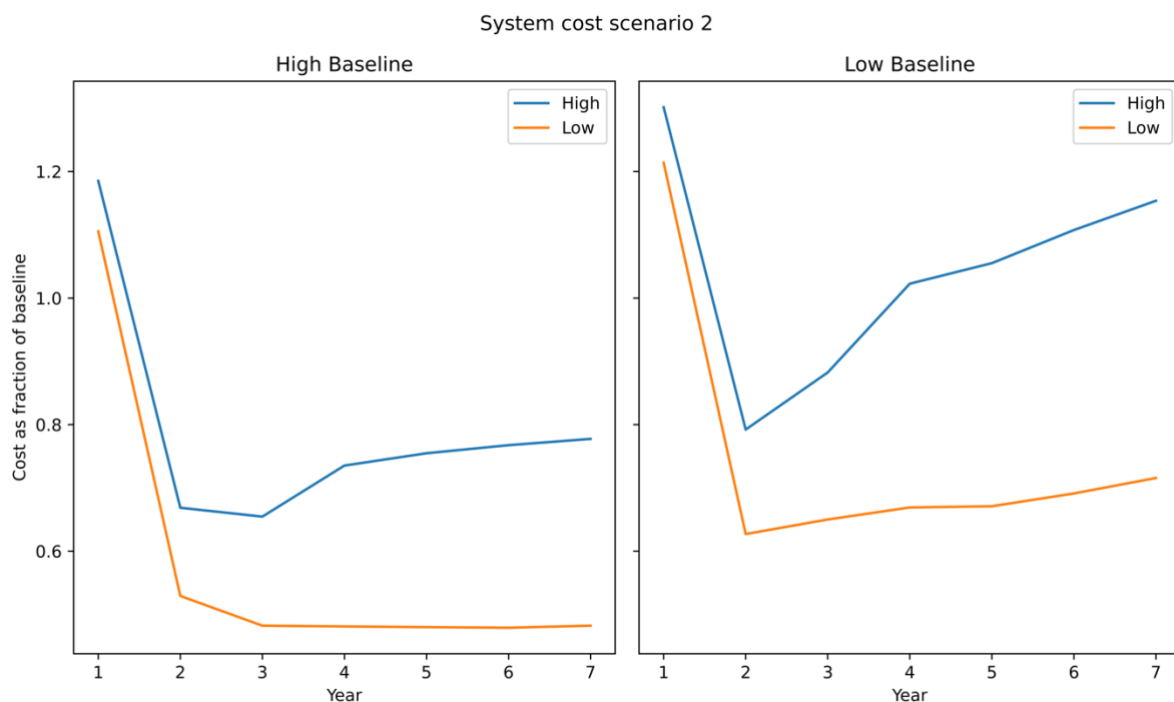
Figure 4-20 System cost in scenario 2 high- and low-growth scene compared to the high- and low-growth baseline scenario. Note that comparing scenario 2 high-scene to scenario 1 low-scene is an unfair basis as they are based on different electricity demand growth. This is also true for scenario 2 low-growth compared to scenario 1 high-growth.

Scenario 3

Overall system cost is lower than the baseline in scenario 3 in all years except year 1. As seen in Figure 4-21 system cost is roughly four times higher than the baseline in year 1 of scenario 3 but sharply decreases to below half the cost in year 2. This signifies that the operational cost of a system without electrical energy imported from the external transmission grid is significantly cheaper than today's configuration. Also apparent from Figure 4-21 is the slight variation between the high- and low-growth baseline comparison and the small difference between the high- and low-growth scene in scenario 3. This seems to further strengthen the benefits of utilizing cheap VRE sources through long time energy storage.
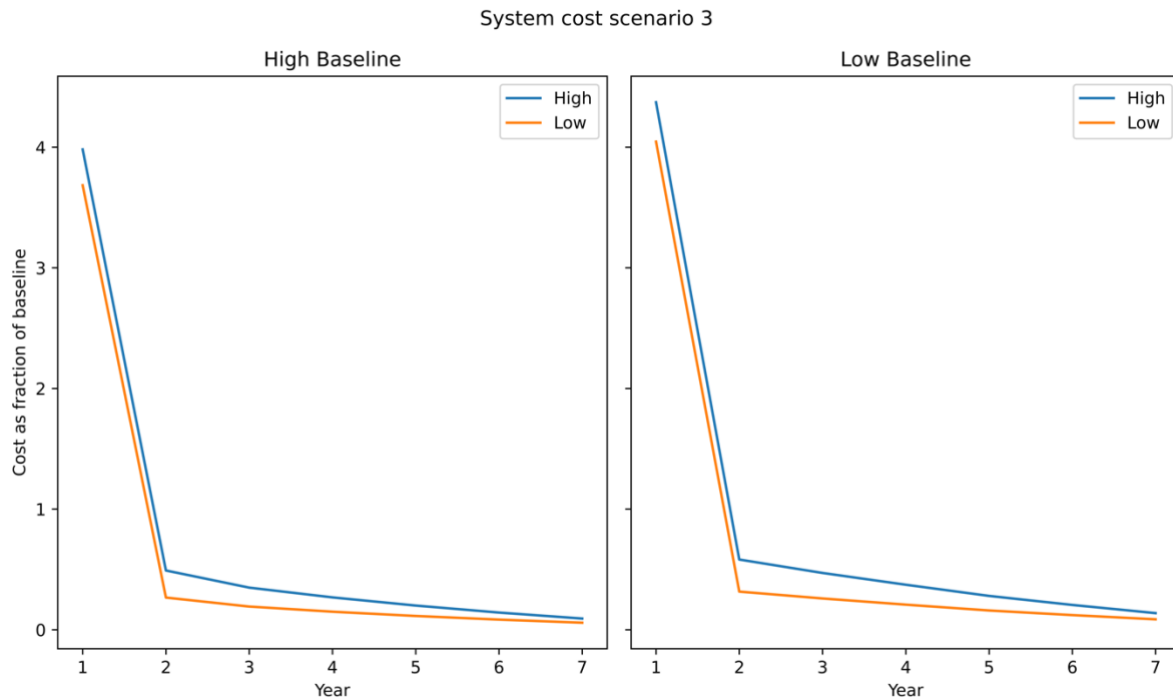
Figure 4-21 System cost in scenario 3 high- and low-growth scene compared to the high- and low-growth baseline scenario. Note the difference in the y-axis compared to Figure 4-20.

4.7 Observations

The model chooses to build all possible expansion solutions in the first year of scenario 2 in both the high- and low-growth scene. Ergo 10MW of wind, 10MW of solar, and 10MW battery capacity are built. This could be done in a more favorable way, as much of the VRE power is curtailed in the early years due to the demand already being met through other sources. This high focus on building all possible power capacity as early as possible is most likely an economic effect based on the value of money throughout the modeling period. The model seeks to maximize the value of each investment to minimize the cost of the system, and as such all investments are made as early as possible to maximize the value of money in an economic system with a flat interest rate. This also becomes apparent in scenario 3 where the model builds a very high power capacity in the first year, to overcome the large energy deficit by not importing power and to make the down payment period as long as possible.

A much higher power capacity than what is reasonable is built in scenario 3 because of the variable nature of the chosen expansion solutions. This could have been reprimanded by implementing more accurate wind and solar variability and forcing the model to comply with real-life VRE constraints. Also allowing the model to build more complex storage solutions could enhance the capability of the network to apprehend variations in power production and uphold a stable power balance. A more accurate representation of wind and solar resources in conjunction with higher complexity battery modeling would increase both VRE penetration and battery utilization.

The original power plants produce much more than actual numbers show and contribute to the power mix to a higher degree than what is reasonable. As the energy capacity of each hydroelectric power plant is set to a fixed number, the model will return to this state at the beginning of each simulation step without calculating the actual inflow. This might skew production numbers as power plants can produce at full power without considering the value of water. With greater insight into the inner workings of the model, this could have been simulated more precisely as there is a variable for inflow mentioned in Chapter 3.2.2. The original generators are also impacted by the variability of the other sources in scenario 2 and scenario 3. This volatility in power production is not favorable for hydroelectric generators and would lead to a very different production pattern than today. Using hydroelectric generators for power balance control is expensive and tends to increase operating costs as variable operation leads to more wear on the machines.

Less imported power in scenario 2 is good and could mean less strain on the grid. But as seen in Figure 4-12 and Figure 4-9 average transmission loss is highest in scenario 2 and transient variability in transmission loss is increased as seen in Figure 4-9. There is less transmission loss on average in the distribution grid in scenario 3, as most of the production is located within each zone.

Demand is consistently met in all scenarios. This is not correct, according to Arva and Tromskraft. In the baseline scenario, non-served hours should be roughly 1500 each year, with most of these in the winter. This could eighter mean that today's system is not optimally operated, or more likely the model is not simulating actual conditions and is confidently wrong on how energy can be distributed.

The battery energy capacity is too low in scenarios 1 and 2. This prohibits favorable utilization of VRE sources or general power balancing and is more applicable for peak load-shaving purposes. In a system with a highly variable power base such as in scenario 2, this lack of energy capacity is harmful to the power balance. Although battery energy capacity is larger in scenario 3, one can see that for the utilization of VRE to be even higher, more storage is necessary. Higher local VRE utilization would also be beneficial for distribution grid stability as less electricity would have to be transported. This can be seen when comparing Figure 4-16 and Figure 4-19. Batteries produce more when more variability is introduced to the system. As seen when comparing Figure 4-14 with Figure 4-18 and Figure 4-19. This comparison shows a clear connection between battery utilization and VRE implementation.

When the model builds 1MW wind turbines in all zones, some of these stay underutilized for a long time when demand takes a longer time to increase. This could have been circumvented by allowing the model to build in smaller installments but would not be realistic as a greater number of small turbines would be more expensive and tedious to construct.

There is a significant difference between the utilization of the small energy source PV and the more prominent energy source of wind. Wind power also shows how zones don't have the same need for local variable production. As minor variations of PV power are easy to handle and balance, the larger variability of wind power proves difficult for small zones to balance and much of this energy ends up curtailed.

In both scenarios 2 and 3, the initial system cost is higher than the baseline but quickly decreases to being cheaper. There is a much more significant difference in cost between high- and low-growth scenes in scenario 2 than in scenario 3. This could be due to the difference in cost between local production and imported power. There is a clear cost advantage to implementing more distributed power production as the cost of operation is significantly lower after year 2 in scenario 3. The high price of imported power compared to distributed VRE is also a good indicator for local industrial actors to implement their own power production as a means to lower their power consumption from the distribution grid increasing open capacity for further industrial growth.

4.8 Limitations

The use of national cost estimates for power capacity expansion, and not actual local data give a skewed financial prospect in the model, proving wind as a highly profitable resource in areas and seasons with low wind capacity. The same is true for solar power. The way variability is modeled for these sources force them to follow different production curves than actual variable sources in the area. This could be mended by implementing local radiation data and wind modeling through for example ArcGIS and Wind Atlas Analysis and Application Program (WAsP) or Weather Research and Forecast (WRF) [78]. Optimally the variable sources would follow daily and yearly production curves. This implementation could lead to more utilization of the batteries in the system, and a more accurate simulation of the power balance in the grid.

Grid capacity might have been modeled higher than what is the actual case for the distribution grid on Senja. The model does not implement voltage control and reactive power balance in the network. Not including these factors make the modeled network more resilient than the existing network.

The model does not consider the value of water and is not limited by occasional years of weak inflow in the hydroelectric reservoirs. A more comprehensive examination of the local inflow for the generators on Senja could have been conducted to give more accurate production data.

The model lacks temporal resolution and technical fidelity to correctly implement the batteries installed today in Senja. There is no insight into voltage correction and reactive power stability, only power balancing over short time periods. If a more comprehensive evaluation of the electrical network was to be implemented, the GenX model could be supplemented by a more technical electrical inspection tool. When constructing the model, long storage batteries could have been set up as a separate option to serve as power-balancing tools.

The model should have the opportunity to build the 1MW turbines in the zones where demand is highest and prioritize where it wants to spend its resources. More insight into where the

model could distribute the curtailed energy would be favorable as system operators could use this information to prioritize where they want to expand network capacity.

The model does not provide hourly price outputs for simulations over multiple years. So, there is no reasonable way to offer levelized cost of electricity values (LCOE). The baseline scenario is highly dependent on the price of imported power. Minor variations in this will have a significant impact on the comparisons of Figure 4-20 and Figure 4-21. More accurate financial data would give a more concise picture of the economic status for each scenario but would come at the cost of structural integrity for the model as more variables would have to be considered.

The model seems prone to calculation errors in scenario 3. As seen in Figure 4-12. The cause of these is unknown.

5 Conclusion

5.1 Summary

A prescriptive analysis is one of the most powerful tools at a decision-makers disposal when an electrical network needs improvement. In this thesis, prescriptive analysis has been used to mathematically optimize an eldering distributional network on the island of Senja in northern Norway. Through a cost-minimizing model based on a bottom-up technical foundation, three scenarios have been simulated from today and through 2030.

The model has proven that the distributional network of Senja can deliver stable and reliable power when operated optimally, with no line capacity expansion.

In scenario 2, the model finds that small implementations of distributed local production can positively impact system capacity and power balance while proving financially competitive. As the means of distributed local energy production in the model include naturally inherent variability, energy storage is paramount for optimal system operation. Increased local production also proves a decrease in strain on the regional network, as imports from the external transmission grid decrease by 14% on average. This is important as the only current connection to the external grid is old and almost at maximum transfer capacity. Countering this improvement in the regional network is the increased strain on the distribution network, as local zones distribute power with each other when there is a large discrepancy between production and demand between zones. This loads the already overloaded radials of the distribution network even more and leads to higher losses in the network than in the baseline scenario. The inherent variability of the distributed local production also impacts the hydroelectric generators on the island, as these must balance the power in the network. Such variable operation of a hydroelectric generator increase wear on the equipment and tends to increase maintenance costs.

Power balance can also be met through energy storage utilization, and the model shows that the increased variability introduced through distributed local production with SRE sources can to some degree be balanced. A 150% increase in battery utilization from the baseline scenario proves that an increase in variability in energy production also increases battery utilization. The final balancing tool in the model is VRE curtailment, where overproduction from variable sources is dumped to balance supply and demand. High curtailment is bad and depicts an overbuilt energy system. This study shows that VRE curtailment is lowest when VRE penetration is relatively low compared to the system load. Overall system cost is lower in scenario 2, with year one as an exception where the initial cost of the system expansion increases cost beyond the baseline scenario.

Island operation has been simulated in scenario 3, with no connection to the external transmission network. In this scenario, considerable amounts of local electrical energy production would have to be built. Still, economic assessment proves a financial incentive as operational costs decrease significantly compared to the baseline scenario. Such high penetration of variable energy sources proves to be very difficult for the electrical network to balance, forcing the model to build enough power capacity to supply all demand even at times when production is at its lowest. This large expansion then tends towards very high curtailment as the energy system is massively overbuilt and fails to utilize most of its resources. Even so, the system cost of energy is substantially lower than the baseline in all years but the first, where the initial cost of the capacity expansion drives prices 500% beyond the baseline scenario.

The study has shown the great potential and some of the shortcomings of prescriptive analytics through GenX. This mathematical optimization tool is an excellent choice when assessing large complex energy systems with many different sources and technologies. When analyzing a smaller system similar to the electrical distribution on Senja the model lacks technical fidelity and some crucial details to grasp the underlying faults in the system.

5.2 Further Work

Use GenX on a larger system. All of northern Norway could be an interesting case, or the entire country with modeling zones based on national price zones. This thesis has concluded that large-scale simulations over multiple years are feasible and can be done in a matter of minutes on a personal computer. Implementing GenX in other secluded parts of the world where island operation is a problem would be interesting but could also be difficult because of the need for high quality data for an accurate model representation.

Another interesting topic would be a more thorough economic analysis of the energy system on Senja based on local assessments of production cost and variability. This assessment should include LOCE calculations and a net present value investigation. Allowing for such an assessment would substantiate a more thorough look into the financial calculations of the model and find a way to assess hourly financial data.

Using GenX in conjunction with more technical electrical assessment tools could give a more holistic insight into the problems present in the electrical network on Senja. Interested parties in this thesis have shown interest in assessing the solutions prescribed by GenX in advanced power-flow software to investigate aspects such as voltage regulation and frequency stability.

5.3 Concluding Remarks

Using an open-source product for academic research will always have drawbacks and advantages. Open-source products usually come with the benefit of being widely adopted, with a large user base to share problems and ideas. This tool did not seem to have a large following, and therefore finding supplemental material to the actual source code and documentation was not easy. Open-source code products are also built to be generalized and used in many different cases. In this case, the chosen analytical tool was too broad for many of the desired assessments posed by interested parties. A more technical configuration with voltage control and reactive power balance would greatly supplement the model. For later studies, this tool would be better applied to larger systems with assessments of a less technical degree.

Appendix A

Code used to generate variability for solar and wind resources. See Chapter 3.2.2.

```python
def gen_random():
    arr1 = np.random.randint(0, 40, 4379).astype(np.float)
    arr2 = np.random.randint(40, 125, 4379).astype(np.float)
    mid = [40, 40]
    i = ((np.sum(arr1 + arr2) + 50) - (40 * 8760)) / 3504
    args = np.argsort(arr2)
    arr2[args[-3504:]] -= i
    return np.concatenate((arr1, mid, arr2))

def gen_random_s():
    arr1 = np.random.randint(0, 15, 4379).astype(np.float)
    arr2 = np.random.randint(15, 100, 4379).astype(np.float)
    mid = [14, 16]
    i = ((np.sum(arr1 + arr2) + 13) - (15 * 8760)) / 3504
    args = np.argsort(arr2)
    arr2[args[-3504:]] -= i
    return abs(np.concatenate((arr1, mid, arr2)))
```

Code used to normalize load data. See Chapter 3.4.1.

```python
CT = pd.DataFrame(CU["Sum_last"].rolling(730,win_type=None).mean())
li = [i for i in range(730)]
CT = CT.drop(li)
NU = CT.apply(lambda x: x/x.max(), axis=0)
```

Code used to separate radials into nodes and add load data. See Chapter 3.4.1 and Chapter 3.4.2.

```python
SILS = []
SVAN = []
STON = []
STRA = []
REST = []
GI1 = []
O1 = []
SI1 = []
LY1 = []
SV1 = []
OS1 = []
SK1 = []
SS1 = []
ST1 = []
SV2 = []
RE = []

for i in ST.values:
    if i[2] == 'SILS 22GI1':
        GI1.append(i[3])
    elif i[2] == 'STRA 2201':
        O1.append(i[3])
    elif i[2] == 'SVAN 22SI1':
        SI1.append(i[3])
    elif i[2] == 'SVAN 22LY1':
        LY1.append(i[3])
    elif i[2] == 'STRA 22SV1':
        SV1.append(i[3])
    elif i[2] == 'STON 22OS1':
        OS1.append(i[3])
    elif i[2] == 'STRA 22SK1':
        SK1.append(i[3])
    elif i[2] == 'SVAN 22SS1':
        SS1.append(i[3])
    elif i[2] == 'STON 22ST1':
        ST1.append(i[3])
    elif i[2] == 'SILS 22SV1':
        SV2.append(i[3])
    else:
        RE.append(i[3])
```

```python
for i in ST.values:
    if i[2] == 'SILS 22GI1':
        SILS.append(i[3])
    elif i[2] == 'STRA 22O1':
        STRA.append(i[3])
    elif i[2] == 'SVAN 22SI1':
        SVAN.append(i[3])
    elif i[2] == 'SVAN 22LY1':
        SVAN.append(i[3])
    elif i[2] == 'STRA 22SV1':
        STRA.append(i[3])
    elif i[2] == 'STON 22OS1':
        STON.append(i[3])
    elif i[2] == 'STRA 22SK1':
        STRA.append(i[3])
    elif i[2] == 'SVAN 22SS1':
        SVAN.append(i[3])
    elif i[2] == 'STON 22ST1':
        STON.append(i[3])
    elif i[2] == 'SILS 22SV1':
        SILS.append(i[3])
    else:
        REST.append(i[3])


sils = sum(SILS)
SILS = []
for i in range(8760):
    SILS.append(sils*NU.iloc[i])
svan = sum(SVAN)
SVAN = []
for i in range(8760):
    SVAN.append(svan*NU.iloc[i])
stra = sum(STRA)
STRA = []
for i in range(8760):
    STRA.append(stra*NU.iloc[i])
ston = sum(STON)
STON = []
for i in range(8760):
    STON.append(ston*NU.iloc[i])
rest = sum(REST)
REST = []
for i in range(8760):
    REST.append(rest*NU.iloc[i])
gi1 = sum(GI1)*0.70
GI1 = []
for i in range(8760):
    GI1.append(gi1*NU['Sum_last'].iloc[i])
o1 = sum(O1)*0.70
O1 = []
for i in range(8760):
    O1.append(o1*NU['Sum_last'].iloc[i])
si1 = sum(SI1)*0.70
SI1 = []
for i in range(8760):
    SI1.append(si1*NU['Sum_last'].iloc[i])
ly1 = sum(LY1)*0.70
LY1 = []
for i in range(8760):
    LY1.append(ly1*NU['Sum_last'].iloc[i])
sv1 = sum(SV1)*0.70
SV1 = []
for i in range(8760):
    SV1.append(sv1*NU['Sum_last'].iloc[i])
os1 = sum(OS1)*0.70
OS1 = []
for i in range(8760):
    OS1.append(os1*NU['Sum_last'].iloc[i])
sk1 = sum(SK1)*0.70
SK1 = []
for i in range(8760):
    SK1.append(sk1*NU['Sum_last'].iloc[i])
ss1 = sum(SS1)*0.70
SS1 = []
for i in range(8760):
    SS1.append(ss1*NU['Sum_last'].iloc[i])
st1 = sum(ST1)*0.70
ST1 = []
for i in range(8760):
    ST1.append(st1*NU['Sum_last'].iloc[i])
sv2 = sum(SV2)*0.70
SV2 = []
for i in range(8760):
    SV2.append(sv2*NU['Sum_last'].iloc[i])
```

Bibliography

[1]   Statistics Norway. "Elektrisitet." https://www.ssb.no/energi-og-industri/energi/statistikk/elektrisitet (accessed 08.05, 2023).

[2]   Smart Senja. "Smart Senja." https://smartsenja.no/en/dokumenter/ (accessed 08.05, 2023).

[3]   Troms kraft nett as, ishavskraft, troms kraft produksjon as, nodes as, enfo as, and eaton electric as, powel as, solbes as, uit – arctic centre for sustainable energy, sjømatindustrien, "Sluttrapportering på konseptutredning: Smartinfrastruktur nord senja.," 2019.

[4]   Sjømatklyngen Senja, "Energiforbruk i sjømatregionen Senja 2016-2030," 2021.

[5]   T. T. Jacobsen, "Distributed Renewable Generation and Power Flow Control to Improve Power Quality at Northern Senja, Norway," Master, Department of Physics and Technology, UiT The arctic university of Norway, Munin.no, 2019.

[6]   K. H. Rochmann, "Network Analysis and Boosting the Distribution to Local Consumers at Northern Senja, Norway with Potential Renewable Generation Using Power Flow Control," Master, Department of Physics and Technology, UiT The arctic university of Norway, Munin.no, 2022.

[7]   I. H. Løvvold, "Pumped Hydropower Conversion and Renewable Hybrid Power Plants at Senja," Master, Department of Physics and Technology, UiT The arctic university of Norway, Munin.no, 2020.

[8]   O. Foldvik Eikeland, F. M. Bianchi, H. Apostoleris, M. Hansen, Y.-C. Chiou, and M. Chiesa, "Predicting Energy Demand in Semi-Remote Arctic Locations," *Energies*, vol. 14, no. 4*, doi: 10.3390/en14040798.

[9]   O. F. Eikeland, F. Maria Bianchi, I. S. Holmstrand, S. Bakkejord, S. Santos, and M. Chiesa, "Uncovering Contributing Factors to Interruptions in the Power Grid: An Arctic Case," *Energies*, vol. 15, no. 1*, doi: 10.3390/en15010305.

[10]   O. F. Eikeland, I. S. Holmstrand, S. Bakkejord, M. Chiesa, and F. M. Bianchi, "Detecting and Interpreting Faults in Vulnerable Power Grids With Machine Learning," *IEEE Access,* vol. 9, pp. 150686-150699, 2021, doi: 10.1109/ACCESS.2021.3127042.

[11]   International Renewable Energy Agency, "World Energy Transitions Outlook 2023: 1.5°C Pathway,," Abu Dhabi,, 2023. Accessed: 2023.

[12]   S. J. Chapman, *Electric machinery fundamentals*, 5th ed. New York: McGraw-Hill, 2012.

[13]   International Energy Agency, "Electricity information," 2022.

[14]   I. Bostan, V. Bostan, V. Dulgheru, A. Gheorghe, I. Sobor, and A. Sochirean, *Resilient Energy Systems: Renewables: Wind, Solar, Hydro*, 1. Aufl. ed. (Topics in safety, risk, reliability and quality). Dordrecht: Dordrecht: Springer Netherlands, 2013.

[15]   C. Ballif, F.-J. Haug, M. Boccard, P. J. Verlinden, and G. Hahn, "Status and perspectives of crystalline silicon photovoltaics in research and industry," *Nature Reviews Materials,* vol. 7, no. 8, pp. 597-616, 2022/08/01 2022, doi: 10.1038/s41578-022-00423-2.

[16]   T. Muneer, E. Jadraque Gago, and S. Etxebarria Berrizbeitia, *The Coming of Age of Solar and Wind Power* (Green Energy and Technology). Cham: Cham: Springer International Publishing AG, 2022.

[17]   P. Schavemaker and L. V. d. Sluis, *Electrical power system essentials*, Second edition. ed. Croydon: John Wiley & Sons, 2017.

[18]   A. S. Blazev, *Power generation and the environment*, 1st. ed. Gistrup: River Publishers, 2021.

[19] J. M. Cimbala, *Advancements in Hydropower Design and Operation for Present and Future Electrical Demand*, B. J. Lewis and J. M. Cimbala, eds., Basel: MDPI - Multidisciplinary Digital Publishing Institute, 2022.

[20] H. Apostoleris, M. Stefancich, and M. Chiesa, "Tracking-integrated systems for concentrating photovoltaics," *Nature energy.,* vol. 1, no. 4, p. 1, 2016, doi: 10.1038/nenergy.2016.18.

[21] C. Maragliano, M. Chiesa, and M. Stefancich, "Point-focus spectral splitting solar concentrator for multiple cells concentrating photovoltaic system," *Journal of Optics,* vol. 17, no. 10, p. 105901, 2015/08/24 2015, doi: 10.1088/2040-8978/17/10/105901.

[22] M. Mokhtar, S. A. Meyers, P. R. Armstrong, and M. Chiesa, "Performance of a 100 kWth Concentrated Solar Beam-Down Optical Experiment," *Journal of Solar Energy Engineering,* vol. 136, no. 4, 2014, doi: 10.1115/1.4027576.

[23] C. S. Solanki, *Solar photovoltaics : fundamentals, technologies and applications*, 3rd ed. PHI Learning, 2015.

[24] H. Apostoleris, S. Sgouridis, M. Stefancich, and M. Chiesa, "Utility solar prices will continue to drop all over the world even without subsidies," *Nature energy.,* vol. 4, no. 10, pp. 833-834, 2019, doi: 10.1038/s41560-019-0481-4.

[25] H. Apostoleris and M. Chiesa, "The role of financing in realizing ultra-low solar electricity prices in the Middle East," *2019 IEEE 46th Photovoltaic Specialists Conference (PVSC),* pp. 0595-0600, 2019, doi: 10.1109/PVSC40753.2019.8980633.

[26] H. Apostoleris, A. Al Ghaferi, and M. Chiesa, "What is going on with Middle Eastern solar prices, and what does it mean for the rest of us?," *Progress in Photovoltaics: Research and Applications,* https://doi.org/10.1002/pip.3414 vol. 29, no. 6, pp. 638-648, 2021/06/01 2021, doi: https://doi.org/10.1002/pip.3414.

[27] D. Choi *et al.*, "Li-ion battery technology for grid application," *Journal of Power Sources,* vol. 511, p. 230419, 2021/11/01/ 2021, doi: https://doi.org/10.1016/j.jpowsour.2021.230419.

[28] The International Panel on Climate Change, "IPCC Sixth Assessment Report," 2022.

[29] J. Chen *et al.*, "Does Renewable Energy Matter to Achieve Sustainable Development Goals? The Impact of Renewable Energy Strategies on Sustainable Economic Growth," *Frontiers in Energy Research,* Review vol. 10, 2022. [Online]. Available: https://www.frontiersin.org/articles/10.3389/fenrg.2022.829252.

[30] X. Wu, W. Zhao, X. Wang, and H. Li, "An MILP-Based Planning Model of a Photovoltaic/Diesel/Battery Stand-Alone Microgrid Considering the Reliability," *IEEE transactions on smart grid,* vol. 12, no. 5, pp. 3809-3818, 2021, doi: 10.1109/TSG.2021.3084935.

[31] P. Breeze, *Wind power generation*, 1st edition. ed. Amsterdam, Netherlands: Academic Press, 2016.

[32] J. Twidell and G. Gaudiosi, *Offshore wind power*. Brentwood: Multi-Science Publ., 2009.

[33] Norges Vassgrads og Energidirektorat. "Om kraftmarkedet og det norske kraftsystemet." https://www.nve.no/reguleringsmyndigheten/kunde/om-kraftmarkedet-og-det-norske-kraftsystemet/ (accessed 2023).

[34] Norges Vassgrads og Energidirektorat. "NVE Atlas." atlas.nve.no (accessed 2023).

[35] Y. Zhang, T. Qian, and W. Tang, "Buildings-to-distribution-network integration considering power transformer loading capability and distribution network reconfiguration," *Energy,* vol. 244, p. 123104, 2022/04/01/ 2022, doi: https://doi.org/10.1016/j.energy.2022.123104.

[36]   P. Kotsampopoulos, *Advancements in Real-Time Simulation of Power and Energy Systems*, O. Faruque and P. Kotsampopoulos, eds., Basel, Switzerland: MDPI - Multidisciplinary Digital Publishing Institute, 2021.

[37]   International Electrotechnical Commission, "Transmission and distribution ", 2018.

[38]   A. Alassi, S. Bañales, O. Ellabban, G. Adam, and C. MacIver, "HVDC Transmission: Technology Review, Market Trends and Future Outlook," *Renewable and Sustainable Energy Reviews,* vol. 112, pp. 530-554, 2019/09/01/ 2019, doi: https://doi.org/10.1016/j.rser.2019.04.062.

[39]   J. Ekanayake, N. Jenkins, K. Liyanage, J. Wu, and A. Yokoyama, *Smart Grid: Technology and Applications*, 2. Aufl. ed. Hoboken: Hoboken: Wiley, 2012.

[40]   S. A. Mansouri, A. Ahmarinejad, E. Nematbakhsh, M. S. Javadi, A. Esmaeel Nezhad, and J. P. S. Catalão, "A sustainable framework for multi-microgrids energy management in automated distribution network by considering smart homes and high penetration of renewable energy resources," *Energy,* vol. 245, p. 123228, 2022/04/15/ 2022, doi: https://doi.org/10.1016/j.energy.2022.123228.

[41]   H. P. Williams, *Model Building in Mathematical Programming*, 5. Aufl.,5th ed. New York: New York: Wiley, 2013.

[42]   F. M. R. Islam, K. A. Mamun, and M. T. O. Amanullah, *Smart Energy Grid Design for Island Countries : Challenges and Opportunities*, 1st 2017. ed. Cham: Springer International Publishing : Imprint: Springer, 2017.

[43]   I. J. Balaguer, Q. Lei, S. Yang, U. Supatti, and F. Z. Peng, "Control for Grid-Connected and Intentional Islanding Operations of Distributed Power Generation," *IEEE Transactions on Industrial Electronics,* vol. 58, no. 1, pp. 147-157, 2011, doi: 10.1109/TIE.2010.2049709.

[44]   M. Short, *Future Smart Grid Systems*, T. Crosbie, M. Al-Greer, and M. Short, eds., Basel, Switzerland: MDPI - Multidisciplinary Digital Publishing Institute, 2021.

[45]   P. Kurzweil, "Chapter 16 - Lithium Battery Energy Storage: State of the Art Including Lithium–Air and Lithium–Sulfur Systems," in *Electrochemical Energy Storage for Renewable Sources and Grid Balancing*, P. T. Moseley and J. Garche Eds. Amsterdam: Elsevier, 2015, pp. 269-307.

[46]   P. Bernard and M. Lippert, "Chapter 14 - Nickel–Cadmium and Nickel–Metal Hydride Battery Energy Storage," in *Electrochemical Energy Storage for Renewable Sources and Grid Balancing*, P. T. Moseley and J. Garche Eds. Amsterdam: Elsevier, 2015, pp. 223-251.

[47]   B. Zakeri and S. Syri, "Electrical energy storage systems: A comparative life cycle cost analysis," *Renewable and Sustainable Energy Reviews,* vol. 42, pp. 569-596, 2015/02/01/ 2015, doi: https://doi.org/10.1016/j.rser.2014.10.011.

[48]   M. o. P. a. Energy. "Kraftmarked og Strømpris." https://www.regjeringen.no/no/tema/energi/stromnettet/kraftmarkedet-og-strompris/id2076000/ (accessed 2023).

[49]   X. Luo, J. Wang, M. Dooner, and J. Clarke, "Overview of current development in electrical energy storage technologies and the application potential in power system operation," *Applied Energy,* vol. 137, pp. 511-536, 2015/01/01/ 2015, doi: https://doi.org/10.1016/j.apenergy.2014.09.081.

[50]   *Advances in Underground Energy Storage for Renewable Energy Sources*. Basel, Switzerland: Basel, Switzerland: MDPI - Multidisciplinary Digital Publishing Institute, 2021.

[51]   S. Rehman, L. M. Al-Hadhrami, and M. M. Alam, "Pumped hydro energy storage system: A technological review," *Renewable and Sustainable Energy Reviews,* vol. 44, pp. 586-598, 2015/04/01/ 2015, doi: https://doi.org/10.1016/j.rser.2014.12.040.

[52]   M. S. Javed, T. Ma, J. Jurasz, and M. Y. Amin, "Solar and wind power generation systems with pumped hydro storage: Review and future perspectives," *Renewable Energy,* vol. 148, pp. 176-192, 2020/04/01/ 2020, doi: https://doi.org/10.1016/j.renene.2019.11.157.

[53]   Norges Vassgrads og Energidirektorat. "Kostnader for kraftproduksjon." https://www.nve.no/energi/analyser-og-statistikk/kostnader-for-kraftproduksjon/ (accessed 2023).

[54]   J. M. G. Sanchez, *Modelling in Mathematical Programming: Methodology and Techniques* (International Series in Operations Research & Management Science). Cham: Cham: Springer International Publishing AG, 2020.

[55]   Y. Jiang and Z. P. Jiang, "Robust Adaptive Dynamic Programming and Feedback Stabilization of Nonlinear Systems," *IEEE Transactions on Neural Networks and Learning Systems,* vol. 25, no. 5, pp. 882-893, 2014, doi: 10.1109/TNNLS.2013.2294968.

[56]   M. Zebarjadi and A. Askarzadeh, "Optimization of a reliable grid-connected PV-based power plant with/without energy storage system by a heuristic approach," *Solar energy,* vol. 125, pp. 12-21, 2016, doi: 10.1016/j.solener.2015.11.045.

[57]   T. Yang, P. Zhang, J. Zhang, H. Ji, and W. Li, "Coordination control for Integrated Solar Combined Cycle thermoelectric coupling," *Energy Reports,* vol. 8, pp. 1313-1325, 2022/07/01/ 2022, doi: https://doi.org/10.1016/j.egyr.2022.02.019.

[58]   L. Vergara-Fernandez, M. M. Aguayo, L. Moran, and C. Obreque, "A MILP-based operational decision-making methodology for demand-side management applied to desalinated water supply systems supported by a solar photovoltaic plant: A case study in agricultural industry," *Journal of Cleaner Production,* vol. 334, p. 130123, 2022/02/01/ 2022, doi: https://doi.org/10.1016/j.jclepro.2021.130123.

[59]   A. Parisio, E. Rikos, and L. Glielmo, "A Model Predictive Control Approach to Microgrid Operation Optimization," *IEEE Transactions on Control Systems Technology,* vol. 22, no. 5, pp. 1813-1827, 2014, doi: 10.1109/TCST.2013.2295737.

[60]   C. Gambella, B. Ghaddar, and J. Naoum-Sawaya, "Optimization problems for machine learning: A survey," *European Journal of Operational Research,* vol. 290, no. 3, pp. 807-828, 2021/05/01/ 2021, doi: https://doi.org/10.1016/j.ejor.2020.08.045.

[61]   D. Pessach, G. Singer, D. Avrahami, H. C. Ben-Gal, E. Shmueli, and I. Ben-Gal, "Employees recruitment: A prescriptive analytics approach via machine learning and mathematical programming," *DECISION SUPPORT SYSTEMS,* vol. 134, JUL 2020, Art no. 113290, doi: 10.1016/j.dss.2020.113290.

[62]   M. Lombardi, M. Milano, and A. Bartolini, "Empirical decision model learning," *ARTIFICIAL INTELLIGENCE,* vol. 244, pp. 343-367, MAR 2017, doi: 10.1016/j.artint.2016.01.005.

[63]   G. C. Souza, "Supply chain analytics," *BUSINESS HORIZONS,* vol. 57, no. 5, pp. 595-605, SEP-OCT 2014, doi: 10.1016/j.bushor.2014.06.004.

[64]   Senja Kommune. "Fakta om Senja." https://www.senja.kommune.no/fakta-om-senja/ (accessed 2023).

[65]   Arva, "Årsrapport og bærekraftsrapport 2021," 2021.

[66]   Arva, "Regional kraftsystemutredelse for område 21," 2022.

[67]   T. k. produksjon. "Våre kraftverk." https://www.tromskraft.no/produksjon/kraftverk (accessed 2023).

[68]   "MIT Energy Initiative and Princeton University ZERO lab. GenX: a configurable power system capacity expansion model for studying low-carbon energy futures n.d. https://github.com/GenXProject/GenX."

[69] J. Bezanson, A. Edelman, S. Karpinski, and V. B. Shah, "Julia: A Fresh Approach to Numerical Computing," *SIAM REVIEW,* vol. 59, no. 1, pp. 65-98, 2017, doi: 10.1137/141000671.

[70] L. Sivertsen, *Elektriske maskiner : oppbygning, virkemåte og drift*, 1. utgave. ed. Bergen: Fagbokforlaget, 2019.

[71] *Gurobi Optimizer Reference Manual*. (2023). [Online]. Available: "https://www.gurobi.com"

[72] C. L. Lara, D. S. Mallapragada, D. J. Papageorgiou, A. Venkatesh, and I. E. Grossmann, "Deterministic electric power infrastructure planning: Mixed-integer programming model and nested decomposition algorithm," *European Journal of Operational Research,* vol. 271, no. 3, pp. 1037-1054, 2018/12/16/ 2018, doi: https://doi.org/10.1016/j.ejor.2018.05.039.

[73] C. Weihrauch, I. Dimov, S. Branford, and V. Alexandrov, "Comparison of the computational cost of a Monte Carlo and deterministic algorithm for computing bilinear forms of matrix powers," in *Computational Science - Iccs 2006, Pt 3, Proceedings*, vol. 3993, V. N. Alexandrov, G. D. VanAlbada, P. M. A. Sloot, and J. Dongarra Eds., (Lecture Notes in Computer Science, 2006, pp. 640-647.

[74] Norges Bank, "Pengepolitisk rapport 1/2023," 2023.

[75] Norges Vassgrads og Energidirektorat. "Mini, Mikro og Småkraftverk." https://www.nve.no/konsesjon/konsesjonsbehandling-av-vannkraft/mini-mikro-og-smaakraftverk/ (accessed 2023).

[76] Statistics Norway. "Regionale Befolkningsframskrivinger." https://www.ssb.no/befolkning/befolkningsframskrivinger/statistikk/regionale-befolkningsframskrivinger (accessed 24.05, 2023).

[77] SciPy. "Window functions." https://docs.scipy.org/doc/scipy/reference/signal.windows.html (accessed 2023).

[78] D. Carvalho, A. Rocha, C. S. Santos, and R. Pereira, "Wind resource modelling in complex terrain using different mesoscale–microscale coupling techniques," *Applied Energy,* vol. 108, pp. 493-504, 2013.